ARL-TN-0976 ● Nov 2019

Polymers for 3-D-Printed Tools at the Point of Need

by Austin Stilling, Erik Grendahl, and Marc Pepi

NOTICES

Disclaimers

ARL-TN-0976 ● NOV 2019

Polymers for 3-D-Printed Tools at the Point of Need

Austin Stilling and Erik Grendahl
High School Extension Program

Marc Pepi
Weapons and Materials Research Directorate, CCDC Army Research Laboratory

REPORT DOCUMENTATION PAGE			*Form Approved* *OMB No. 0704-0188*

1. REPORT DATE *(DD-MM-YYYY)*	**2. REPORT TYPE**	**3. DATES COVERED (From - To)**
November 2019	Technical Note	September 17, 2019–August 18, 2019

4. TITLE AND SUBTITLE Polymers for 3-D-Printed Tools at the Point of Need	**5a. CONTRACT NUMBER**
	5b. GRANT NUMBER
	5c. PROGRAM ELEMENT NUMBER
6. AUTHOR(S) Austin Stilling, Erik Grendahl, and Marc Pepi	**5d. PROJECT NUMBER**
	5e. TASK NUMBER
	5f. WORK UNIT NUMBER
7. PERFORMING ORGANIZATION NAME(S) AND ADDRESS(ES) CCDC Army Research Laboratory ATTN: FCDD-RLW-MD Aberdeen Proving Ground, MD 21005-5069	**8. PERFORMING ORGANIZATION REPORT NUMBER** ARL-TN-0976
9. SPONSORING/MONITORING AGENCY NAME(S) AND ADDRESS(ES)	**10. SPONSOR/MONITOR'S ACRONYM(S)**
	11. SPONSOR/MONITOR'S REPORT NUMBER(S)

12. DISTRIBUTION/AVAILABILITY STATEMENT

Approved for public release; distribution is unlimited.

13. SUPPLEMENTARY NOTES

Mentor: Marc Pepi, WMRD

ORCID ID(s): Marc Pepi, 0000-0003-0691-5925

14. ABSTRACT

The use of 3-D-printed tools with locally available polymers has the potential to increase efficiency and operational readiness on the battlefield. Currently, the US military has plastic 3-D-printing capabilities at the point of need, but only a limited choice of polymers. This effort summarizes the work of two Weapons and Materials Research Directorate–sponsored student projects and compares many different types of common 3-D-printable polymers to determine which one may be best suitable for the harsh conditions and austere environments associated with forward-operating bases. These polymers were subjected to mechanical and environmental testing for the purpose of characterizing and ranking. Post-fracture optical microscopy was undertaken to better understand the failure modes associated with each of the different polymers.

15. SUBJECT TERMS

3-D-printing, additive manufacturing, polymer processing, point-of-need manufacturing, mechanical testing

16. SECURITY CLASSIFICATION OF:			**17. LIMITATION OF ABSTRACT**	**18. NUMBER OF PAGES**	**19a. NAME OF RESPONSIBLE PERSON**
					Marc Pepi
a. REPORT	**b. ABSTRACT**	**c. THIS PAGE**	UU	56	**19b. TELEPHONE NUMBER (Include area code)**
Unclassified	Unclassified	Unclassified			410.306.0848

Standard Form 298 (Rev. 8/98)
Prescribed by ANSI Std. Z39.18

Contents

List of Figures

List of Tables

Acknowledgments

The students and their mentor would like to thank Nicole Zander (US Army Combat Capabilities Development Command Army Research Laboratory [CCDC ARL]) for her guidance and thorough technical review of this report, as well as providing support work associated with this research. In addition, the following personnel provided support to the research done by these students and should also be acknowledged: Maggie Gillan (formerly CCDC ARL), Alicia Farrell (CCDC ARL), Andrew D'Onofrio (Aberdeen Test Center), Faheem Muhammed (formerly CCDC ARL), Jennifer Sietins (CCDC ARL), Lawrence Holmes (formerly CCDC ARL), Kevin Hart (formerly CCDC ARL), and Michael Zipay (Joppatowne High School).

1. Introduction

This work was part of a Joppatowne High School Capstone project for Austin Stiller, with subsequent characterization performed by US Army Combat Capabilities Development Command (CCDC) Army Research Laboratory (ARL) summer student Erik Grendahl, and focuses on the following plastics: acrylonitrile butadiene styrene (ABS), polylactic acid (PLA), glycol modified polyethylene terephthalate (PET-G), recycled PET, recycled polyethylene terephthalate (rPET) recycled ABS, and polycarbonate (PC). All of these plastics have their own benefit, but the objective was to determine which polymer offered the best collective properties for use in harsh and austere environments. To determine the overall effectiveness of each of these plastics, several tests were performed, including tensile, impact, and three-point bend testing. In addition, UV-light exposure testing and water immersion testing were performed in anticipation to the conditions that may be found on the battlefield.

2. Background

The US military is embracing the use of 3-D printing and additive manufacturing (AM) at the point of need to improve operational readiness and reduce the logistics tail required to get spare parts to the battlefield. The US Marines have increased their exploration of AM to quickly replace parts for weapons, vehicles, and equipment.[1] An article highlighted a scenario, where the Marines at the Mountain Warfare Training Center (MWTC) printed snow boot clips, which often break due to the harsh usage conditions. If the Marine has extra 3-D-printed clips in their pockets, the mission is not compromised. The US Navy experienced a similar situation, when an aircraft valve broke while the pilot was waiting for takeoff in 2010.[2] If the airbase had had 3-D-printing capabilities, the pilot could have taken off that day or the next, instead of waiting weeks for the replacement part to arrive. The advantages of 3-D printing at or near the point of need can be summed up in the following paragraph[3]:

> Imagine a company or brigade able to produce repair parts on the battlefield. The Army alone spends billions of dollars buying parts every year. Every Army unit carries large parts stockpiles to keep rolling. This is costly and adds a huge burden to a unit as it deploys and in moving around the battlefield. A unit can't carry everything, and it's very difficult to predict what parts will be needed, so the Army uses various methodologies to figure out the most important ones on hand, balancing against cost and bulk. When a unit needs a part it doesn't have,

> equipment can sit for weeks until a replacement part is shipped all the way from a depot or the manufacturer. Worse yet, sometimes the part isn't available at all, triggering a potentially lengthy acquisition process. This problem has increasingly plagued the US military. Fewer manufacturers are interested in producing small batches of specialized military items for the fleets that have dwindled from their Cold War expanse. The explosion of unique, constantly evolving low-density equipment used in Iraq and Afghanistan has exacerbated this issue.

To combat this problem, the US Army has deployed polymer 3-D printers at the point of need. The Army Rapid Equipping Force (REF) has sent Expeditionary Laboratories (ExLabs) overseas to counter these capability gaps. These "labs" (representative shown in Fig. 1)[4] contain 3-D printers and milling machines.

Fig. 1 US Army REF ExLab[4]

More recently, the US Army has sent Rapid Fabrication (RFAB) units overseas for testing. For this testing, the 2nd Sustainment Brigade at Camp Humphreys, South Korea, was chosen. According to Chief Warrant Officer Dewey Adams,[5] "The quick turnaround time from design to printing, which ranges from 2 h to a few days, and the ability to deploy the facility anywhere and start producing parts within an hour makes RFAB a boon on the battlefield". Figure 2 shows a 3-D-printed Humvee ignition switch printed in the RFAB.

Fig. 2 A 3-D-printed Humvee ignition switch printed in the RFAB[5]

3. Test Plan

The objective of this effort was to provide a ranking of the polymers that may be available at the point of need, in terms of mechanical and physical properties, and with the anticipation of these parts being utilized in a harsh and austere environment. The thermoplastic polymers chosen for this study included ABS, PLA, PET, recycled PET, PET-G, recycled ABS, and PC. Most of these are traditional 3-D-printing polymers; the idea to use recycled polymers was predicated on the fact that recycling efforts may be undertaken at forward-operating bases (FOBs) to make these polymers available for 3-D printing.

3.1 Polymers Chosen for this Study

ABS is common to the injection molding industry, composing such toys as LEGO building blocks. ABS is best suited where strength, ductility, flexibility, shock resistance, machinability, and thermal stability are required (capable from –20 to 80 °C); however, it is more prone to warping.[6–8] PLA is biodegradable and a popular bioplastic derived from cornstarch or sugarcane. PLA takes advantage of lower printing temperatures, but has the tendency to slightly shrink after 3-D printing.[7] It is very rigid and strong, but also brittle.[8] The fact that it could deteriorate when in prolonged contact with water probably precludes this material from being of use in harsh environments, but it was used in this study for property comparison. PET is commonly used for commercial water bottles and is a good choice for parts that will be in contact with food. The material is fairly rigid and has good chemical resistance, humidity resistance, and abrasion resistance.[7,8] PC is a high-strength polymer designed for engineering applications; however, it is prone to absorbing moisture and is UV sensitive.[7,8] A qualitative listing of properties were found in work by 3D Matter[8] and are shown in Fig. 3. Spider plots of the properties of these materials are shown in Fig. 4.[8]

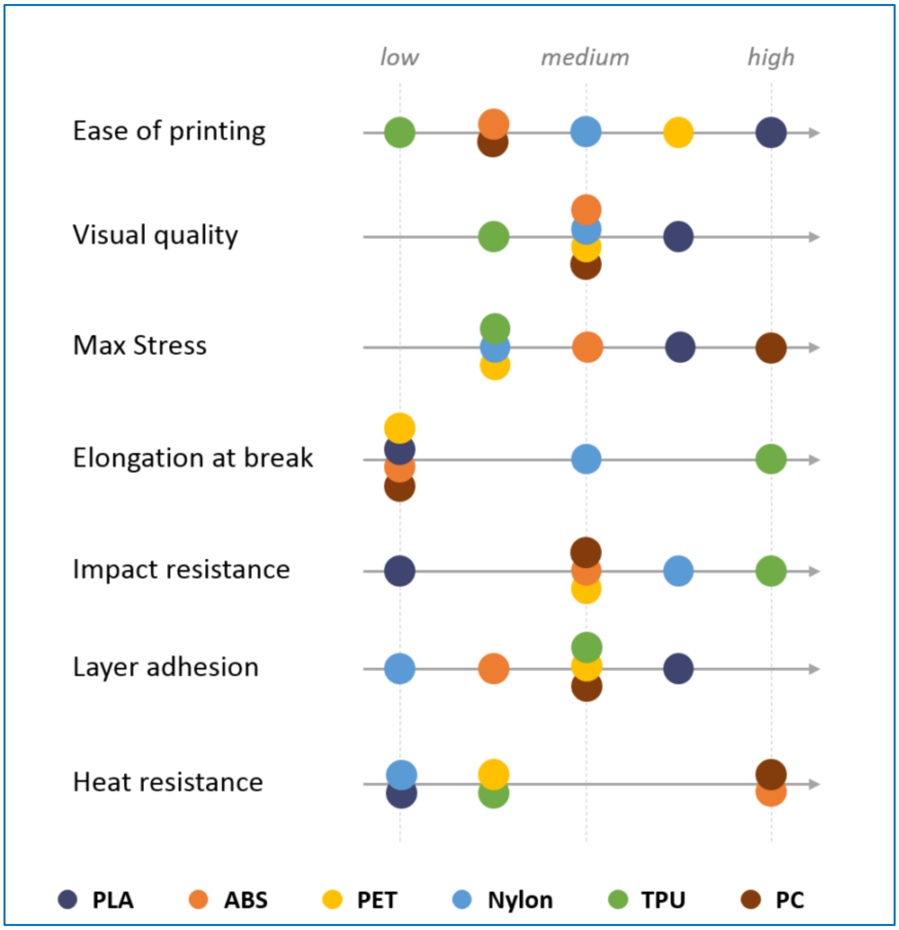

Fig. 3 Properties of common 3-D printing polymers (image used with approval from https://www.3dhubs.com/knowledge-base/fdm-3d-printing-materials-compared[8]). Of the polymers listed, ABS, PLA, PET, and PC were compared in this study.

Fig. 4 Spider plots of the properties of common 3-D-printing polymers (image used with approval from https://www.3dhubs.com/knowledge-base/fdm-3d-printing-materials-compared[8])

3.2 Test Specimens

Mechanical test specimens were printed on the Flash Forge Dreamer 3-D-printer, to include tensile, Charpy impact, and three-point bend tests. Tensile and three-point bend specimens were subjected to UV-light exposure and water immersion testing to compare results to the as-printed specimens. The specimens were printed using digital files derived from the ASTM standards for each specimen (ASTM E8 tensile specimens,[9] ASTM D6110 Charpy impact specimens,[10] and ASTM D790 three-point bend specimens[11]). The .stl files of both the tensile and impact specimens are shown in Figs. 5 and 6, using View 3-D software (the three-point bend specimen design was a simple flat bar and is not included). Figure 7 shows representative tensile specimens made from each polymer, while Fig. 8 shows representative impact specimens and Fig. 9 shows representative three-point bend specimens.

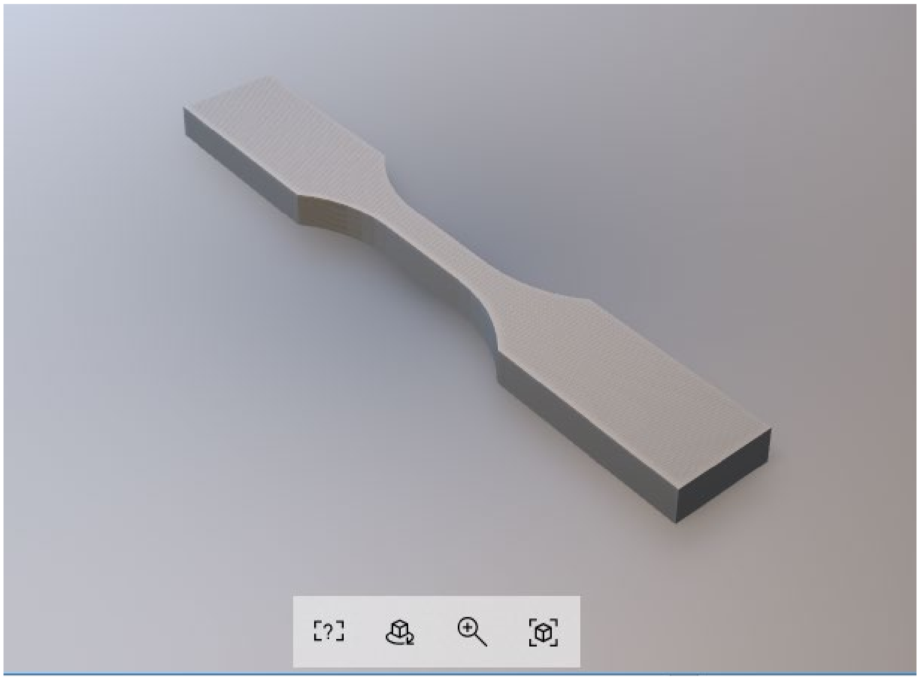

Fig. 5 .stl file of the ASTM E8 tensile specimen used for testing

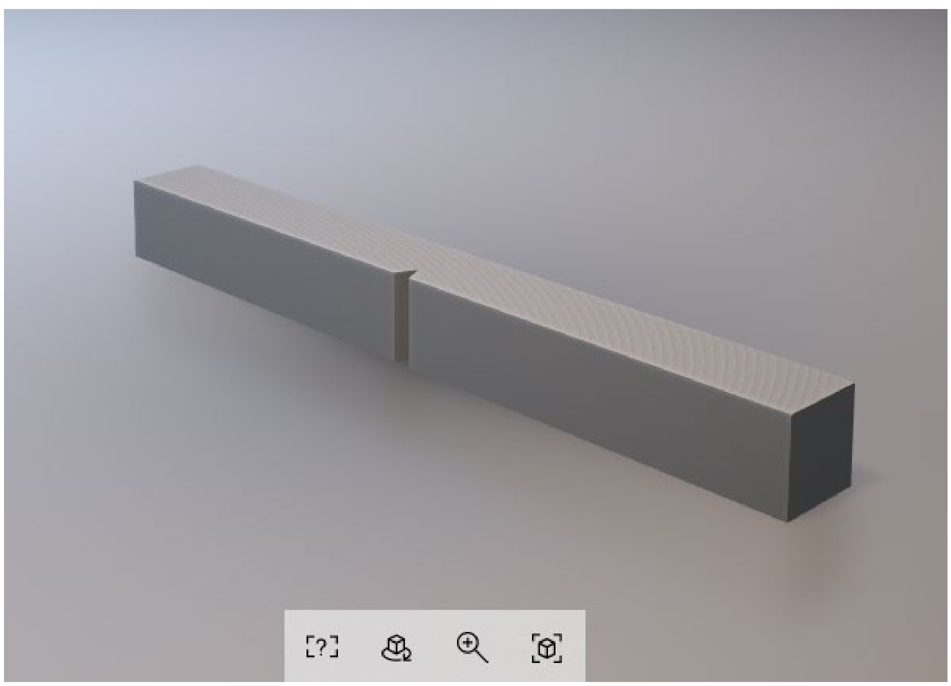

Fig. 6 .stl file of the ASTM D6110 impact specimen used for testing

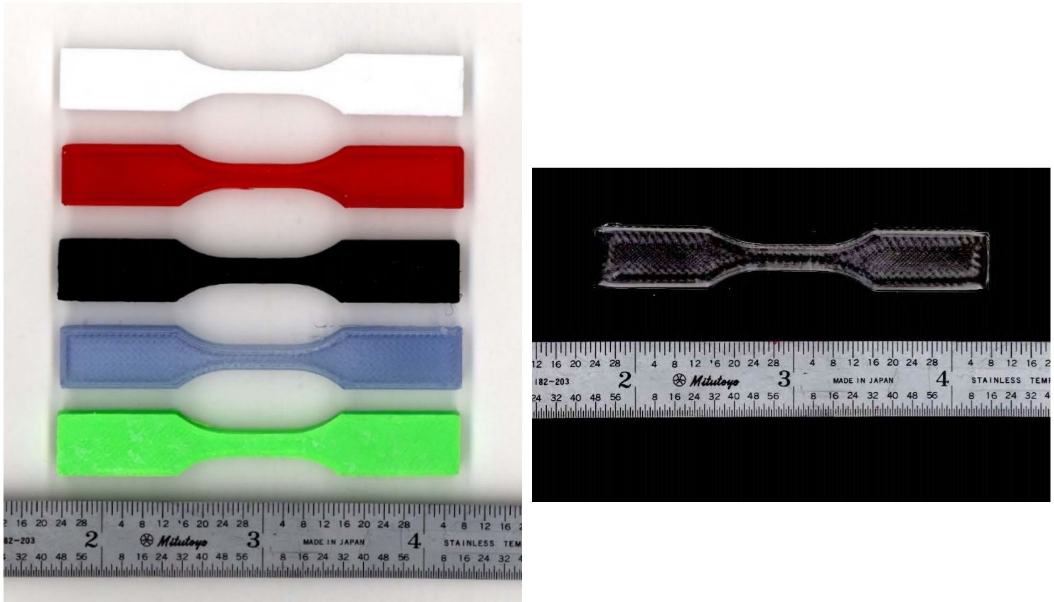

Fig. 7 Representative 3-D-printed tensile specimens printed in PLA, PET-G, rABS, rPET, ABS (top to bottom), and PC (shown in separate photo on right for better contrast)

Fig. 8 Representative 3-D-printed impact specimens printed in PLA, PET-G, rABS, rPET, ABS (top to bottom in top photo), and PC (shown in bottom photo for better contrast)

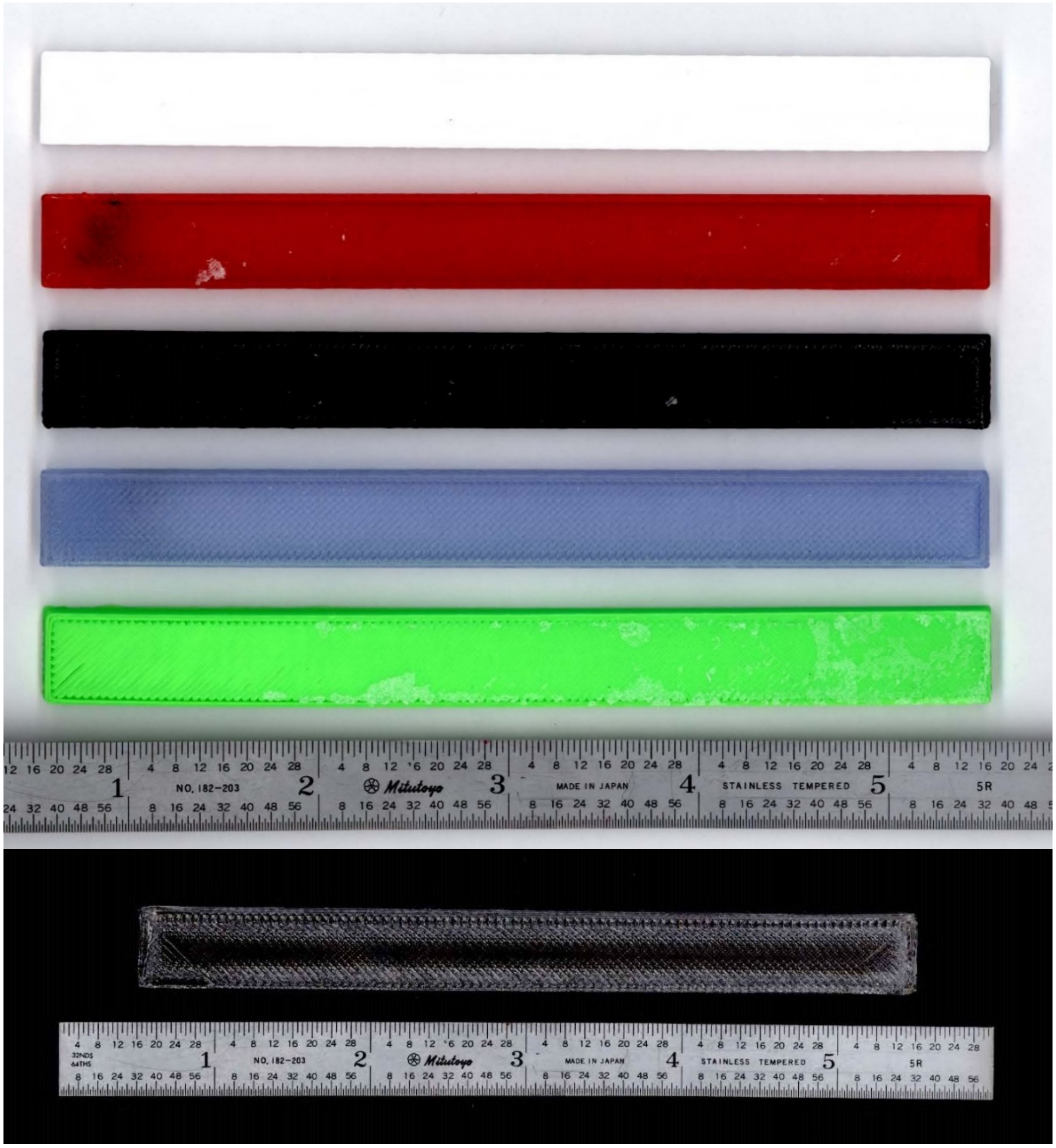

Fig. 9 Representative 3-D-printed three-point bend specimens printed in PLA, PET-G, rABS, rPET, ABS (top to bottom in top photo), and PC (shown in bottom photo for better contrast)

3.3 Observations of Test Specimens in the As-Printed Condition

A couple observations were made regarding the 3-D-printed specimens. For one, it appeared that one side of each of the specimens was rougher than the other. The smoother side was determined to be the side against the build plate during printing, according to the operator (see representative example in Fig. 10). Other anomalies, such as that shown in Fig. 11 (representative ABS specimen), show excess plastic running along the gage section.

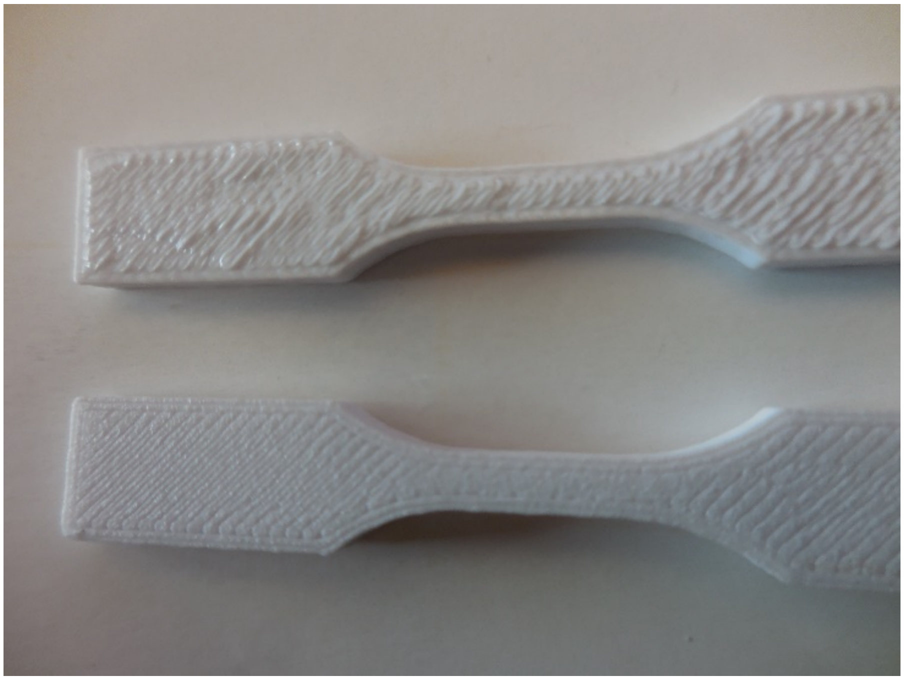

Fig. 10 Representative 3-D-printed specimen showing "rough" vs. "smooth" surface. This is a PLA tensile specimen.

Fig. 11 Representative 3-D-printed specimen showing excess polymer along the gage section (this specimen was not used for testing)

In addition, the PC specimens showed shrinkage and curling at the ends as a result of cooling, as shown in Fig. 12. This can occur of the polymer is cooled too quickly. It was determined that this anomaly was far enough away from the center impact point to ensure the test results would not be affected.

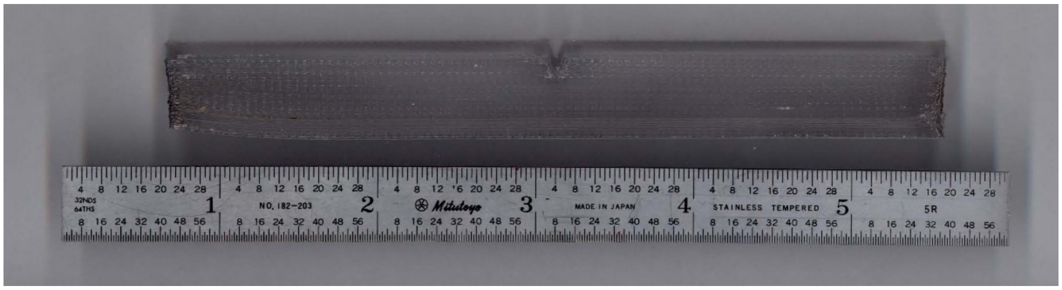

Fig. 12 Representative 3-D-printed PC impact specimen showing curling and shrinkage at the ends.

4. Test Results

A number of tensile and three-point bend specimens were subjected to UV-light exposure and water immersion testing, to compare to the as-printed specimens. Impact specimens were not subjected to these tests, because it was determined that the high strain rate of this test would render no significant change in results.

4.1 UV-Light Exposure Testing

Specimens were tested in accordance with ASTM G154[12] and ASTM G151[13] to determine whether UV exposure would degrade the candidate polymers. A QUV unit (Fig. 13) was used, which is equipped with fluorescent bulbs that emit light at a high intensity in the UV range (340 nm). The test duration for these specimens was 500 h, using typical cycles of 8 h of light at 60 °C, followed by darkness at 50 °C with a light intensity of 0.77 W/m^2. The specimen setup is shown in Fig. 14. Figures 15 and 16 show the discoloration and bending noted on specimens as a result of this testing.

Fig. 13 QUV equipment used for UV exposure testing

Fig. 14 Test setup used within the QUV equipment (tensile specimens on right; three-point bending specimens on left)

Fig. 15 Bending and discoloration of tensile specimens as a result of UV exposure

Fig. 16 Bending and discoloration of three-point bend specimens as a result of UV exposure. Samples deemed to have excessive bending were not tested.

4.2 Water Immersion Testing

A number of tensile specimens were tested in accordance with ASTM D2842[14] to determine whether potential water intake would degrade the candidate polymers. The specimens were preconditioned in an oven for 24 h at 50 °C, and during cooling, the specimens were further dehydrated using a desiccator. The specimens were subsequently weighed to the nearest 0.001 g, per the governing specification.

Immediately after, the specimens were submerged in distilled water for 24 h and then weighed (the specimens were patted dry before weighing). This process was repeated every 7 days after the initial 24 h. Figure 17 shows the test setup used to immerse the specimens in water. As the data in Table 1 (graphically depicted in Figs. 18–22) show the rABS, PET-G, and rPET specimens exhibited the most weight gain as a result of water immersion testing (calculated as the difference between Day 21 specimen weight compared to the original specimen weight), followed by PLA and ABS (the PC was not subjected to this testing, as there was not enough material existed for 3-D printing).

Fig. 17 Test setup for water immersion testing. Foil was needed to keep the specimens submerged.

Table 1 Water immersion results: weight gain standard deviation

Day	ABS (green)			ABS-recycled (black)		
	Specimen 1	Specimen 2	Specimen 3	Specimen 1	Specimen 2	Specimen 3
1	1.35546	1.61218	1.58230	1.64292	1.66171	1.65353
7	1.36821	1.61818	1.58465	1.66198	1.67850	1.67067
14	1.37212	1.62127	1.58649	1.66672	1.68328	1.67507
21	1.37284	1.62303	1.58810	1.66845	1.68566	1.67782
Average	1.36716	1.61867	1.58539	1.66002	1.67729	1.66927
Std. Dev.	0.0080593	0.0047655	0.002493	0.011722	0.010803	0.010900
Difference	0.01738	0.01085	0.00580	0.02553	0.02395	0.02429
	PET-G (red)			PET-recycled (blue)		
1	1.87659	1.87424	1.88783	1.94352	1.91568	1.93253
7	1.89456	1.89635	1.90072	1.96165	1.93929	1.95378
14	1.90434	1.90568	1.90586	1.96645	1.95751	1.95739
21	1.91087	1.90978	1.90560	1.96662	1.94738	1.96046
Average	1.89659	1.89651	1.90000	1.95956	1.93997	1.95104
Std. Dev.	0.014923	0.015876	0.008452	0.010939	0.017823	0.012638
Difference	0.03428	0.03554	0.01777	0.02310	0.03170	0.02793
	PLA (white)					
1	2.01423	2.00545	2.01285			
7	2.02645	2.01799	2.02526			
14	2.02926	2.02008	2.02814			
21	2.03001	2.02130	2.02889			
Average	2.02499	2.01621	2.02379			
Std. Dev.	0.007334	0.007299	0.007456			
Difference	0.01578	0.01585	0.01604			

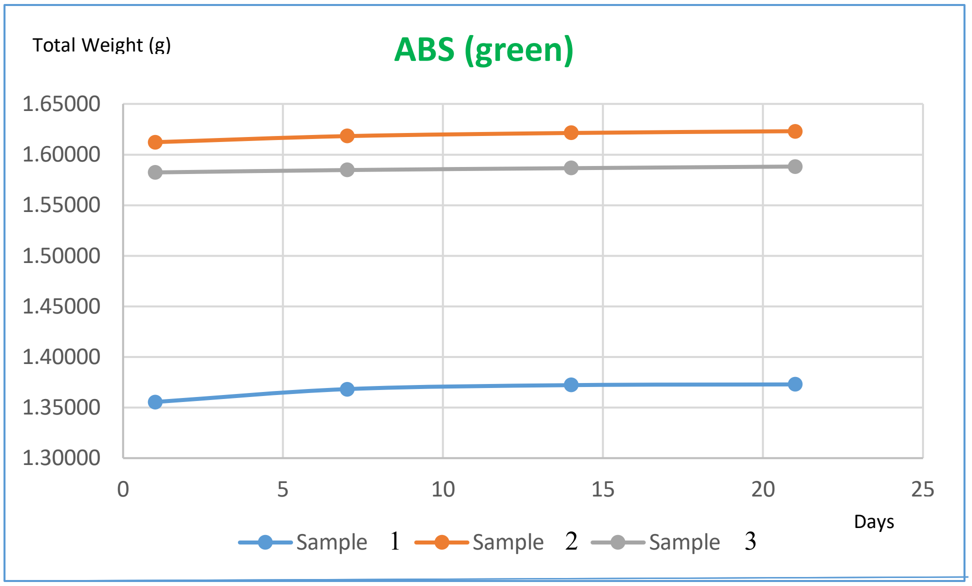

Fig. 18 Water immersion results for three ABS specimens

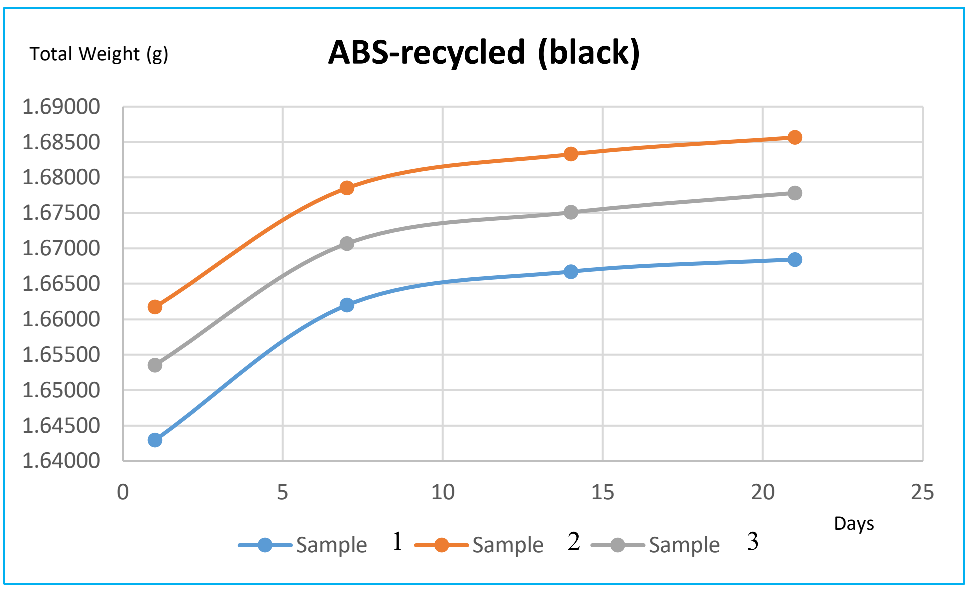

Fig. 19 Water immersion results for three rABS specimens

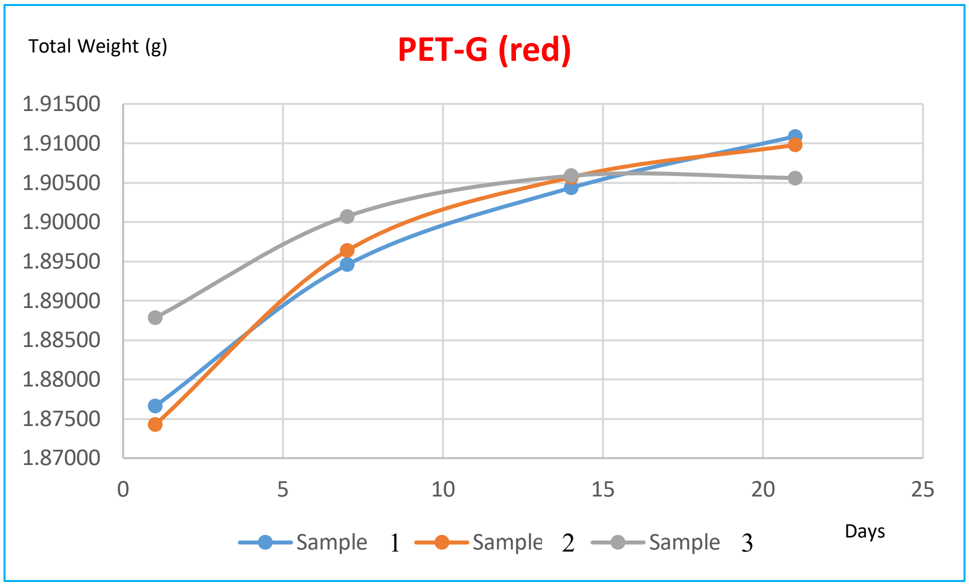

Fig. 20 Water immersion results for three PET-G specimens

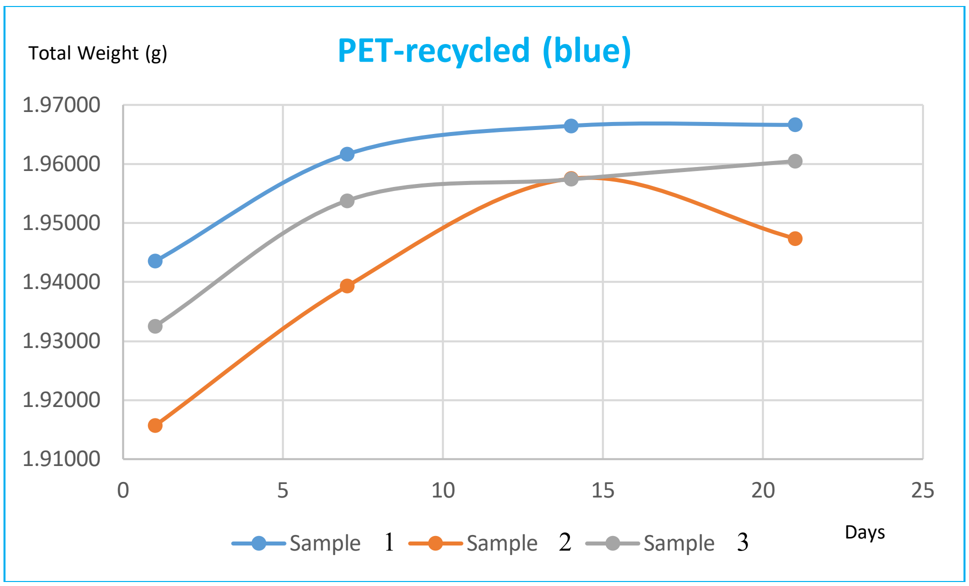

Fig. 21 Water immersion results for three rPET specimens

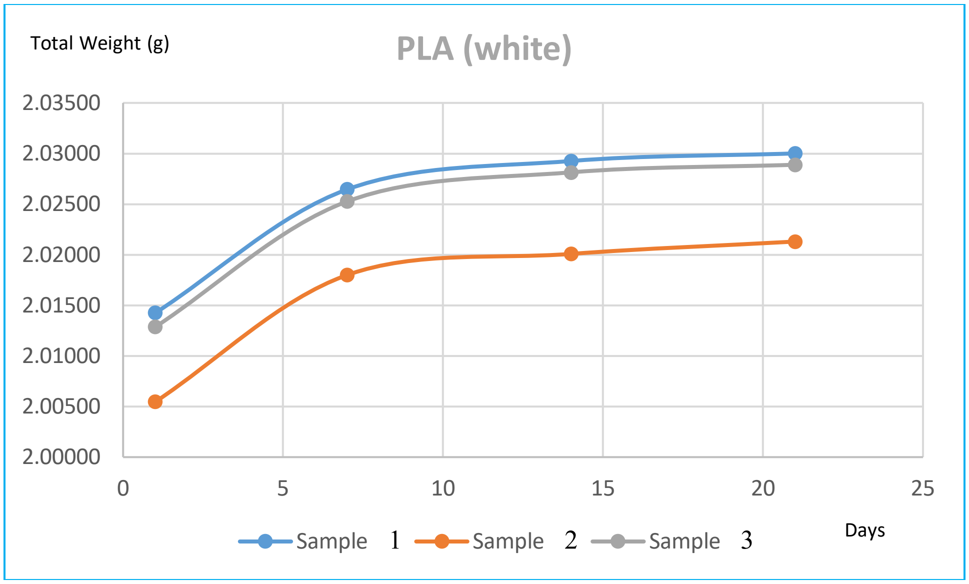

Fig. 22 Water immersion results for three PLA specimens

4.3 Tensile Testing

Tensile testing was performed on an Instron Model 1125 electromechanical test machine in accordance with ASTM E8[9] to determine the effects of UV exposure and water immersion on final results. Yield to a 0.2% offset was measured and a loading rate of 5 mm/min was used for all testing. Figure 23 shows a representative tensile specimen within the grips of the equipment awaiting pull testing. The ultimate tensile strength (UTS) was calculated as the maximum load achieved divided by the cross-sectional area of the gage section; obviously, a stronger material will exhibit a higher UTS. The elastic modulus was calculated by dividing the stress by the strain; a stiffer material will exhibit a higher elastic modulus. The results of tensile testing are listed in Fig. 24 (UTS) and Fig. 25 (elastic modulus). Note that the PET-G and rPET specimens subjected to UV exposure could not be tested due to the extent of distortion. Pneumatic grips were not utilized.

Overall, water immersion did not seem to deleteriously affect the tensile properties; in some cases, properties appeared to be improved with the samples subjected to water immersion. However, the UV-treated specimens seems to exhibit lower tensile properties across the board. The following is the order of decreasing UTS: PLA, PET, PC, rPET, ABS, and rABS. The following is the order of decreasing elastic modulus: PLA, PET, PC, rPET, ABS, and rABS. This seems to contradict Giang,[6] who stated that ABS and PLA have similar tensile strengths.

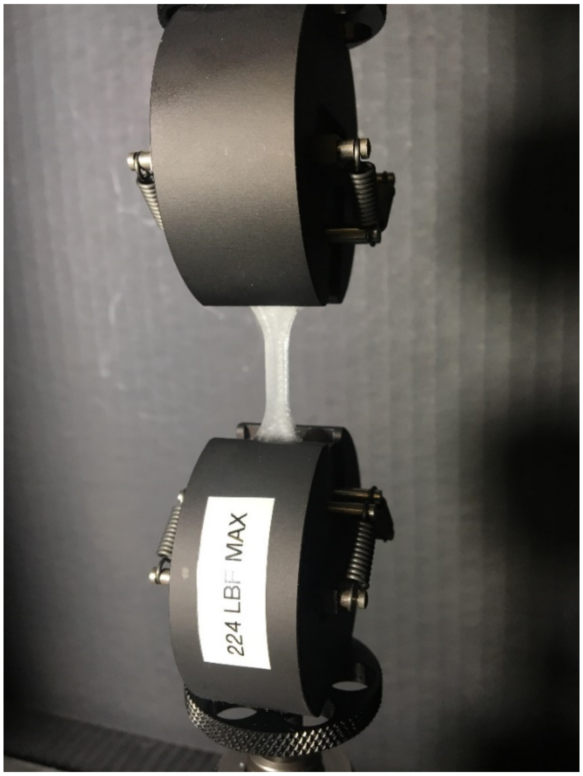

Fig. 23 A representative tensile specimen within the grips of the tensile test machine awaiting pull testing

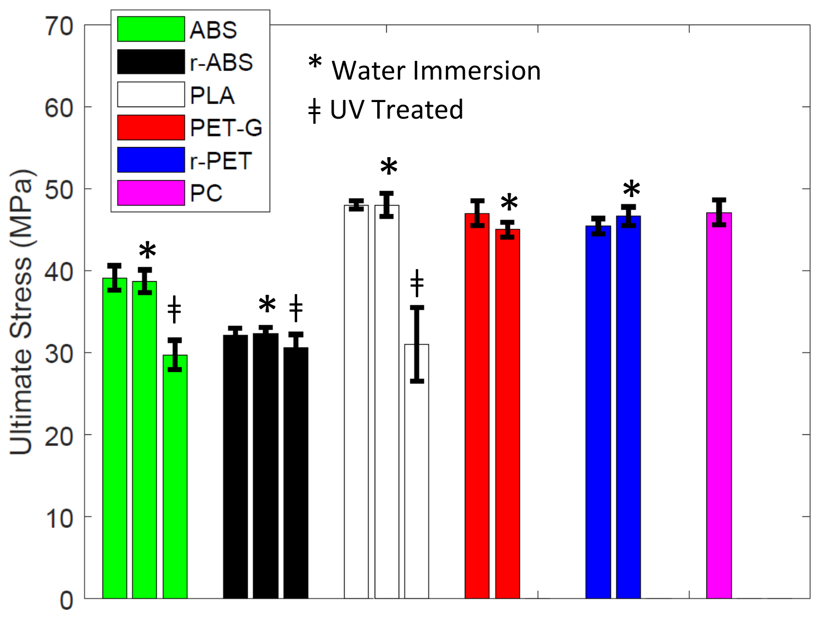

Fig. 24 Tensile results comparing UTS of each sample in the following conditions: as-printed, water immersed (*) and UV exposed (ǂ). Note: Not enough PC specimens were made for UV testing.

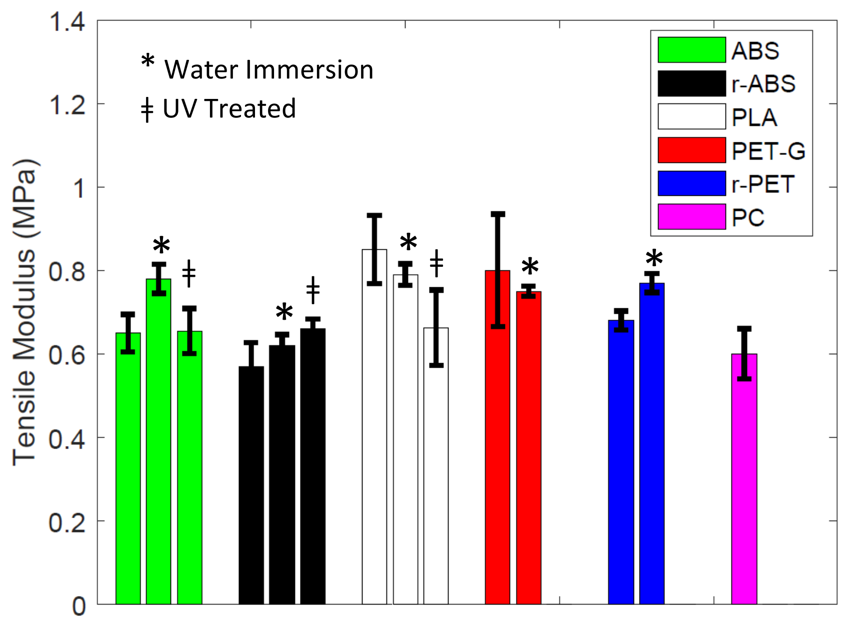

Fig. 25 Tensile results comparing elastic modulus of each sample in the following conditions: as-printed, water immersed (*), and UV exposed (ǂ). Note: Not enough PC specimens were made for UV testing.

4.4 Charpy Impact Testing

Charpy impact testing was performed in accordance with ASTM D6110[10] to determine which plastic exhibited the best energy absorption. Testing was conducted on a benchtop instrumented Instron POE 2000 pendulum impact tester, with a pendulum weight of 4.82 kg, and a tup calibration factor of 2660 N. A typical test setup is shown in Fig. 26. The specimens were required to be centered within the test fixture before release of the pendulum. As the graphs in Figs. 27–32 show, there was much scatter in the results, even within the same material group (see tabulated results in Table 2). Although additional specimens would be needed to confirm trends, the following is the order of decreasing energy to failure: rABS, ABS, PLA, rPET, PET-G, and PC. It was interesting to note that the recycled materials performed better than the virgin materials.

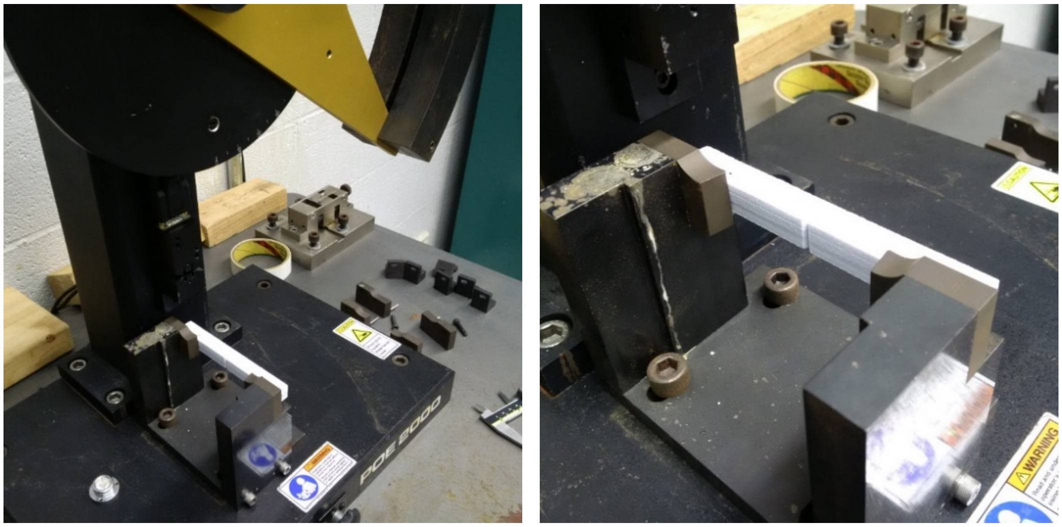

Fig. 26 Test setup for Charpy impact testing (PLA impact specimen)

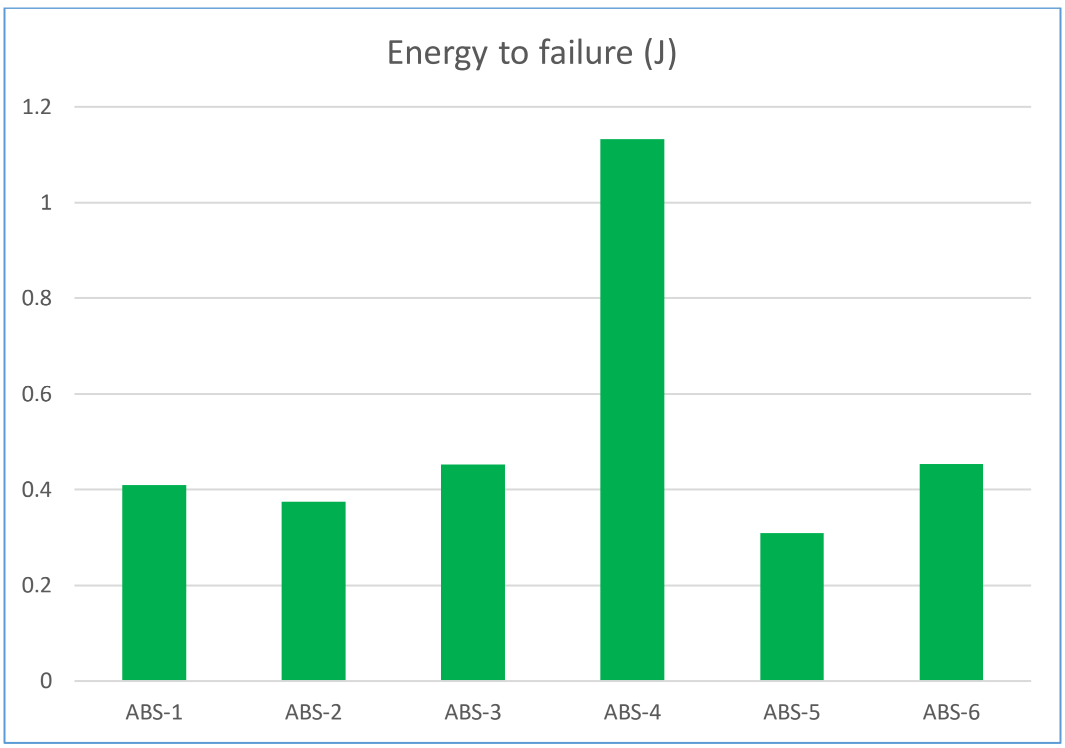

Fig. 27 Impact results of the ABS specimens

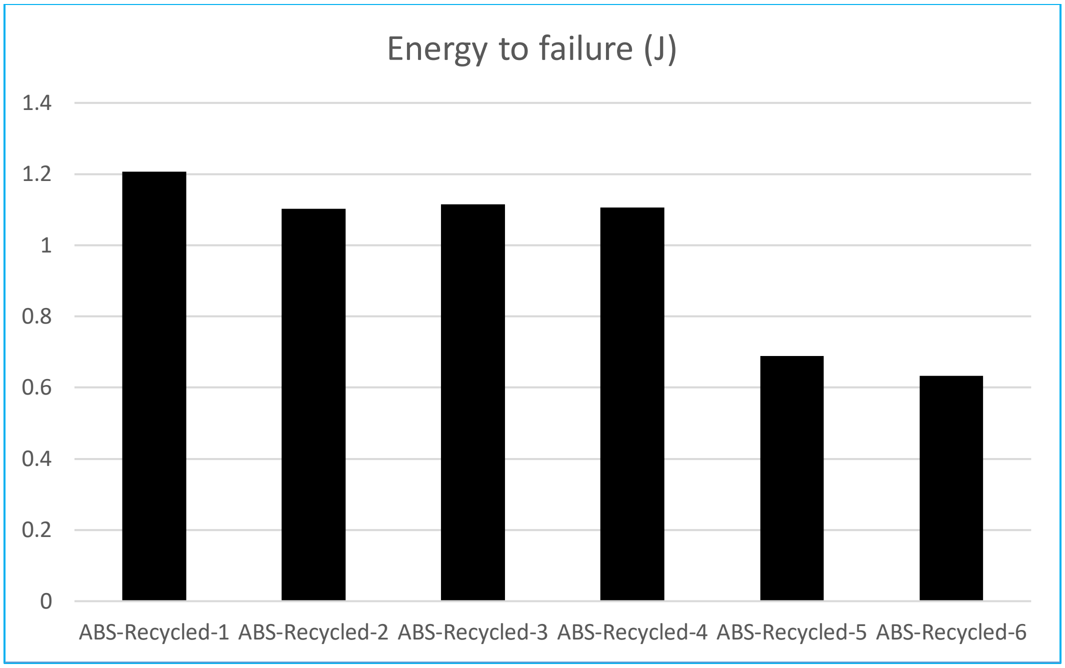

Fig. 28 Impact results of the rABS specimens

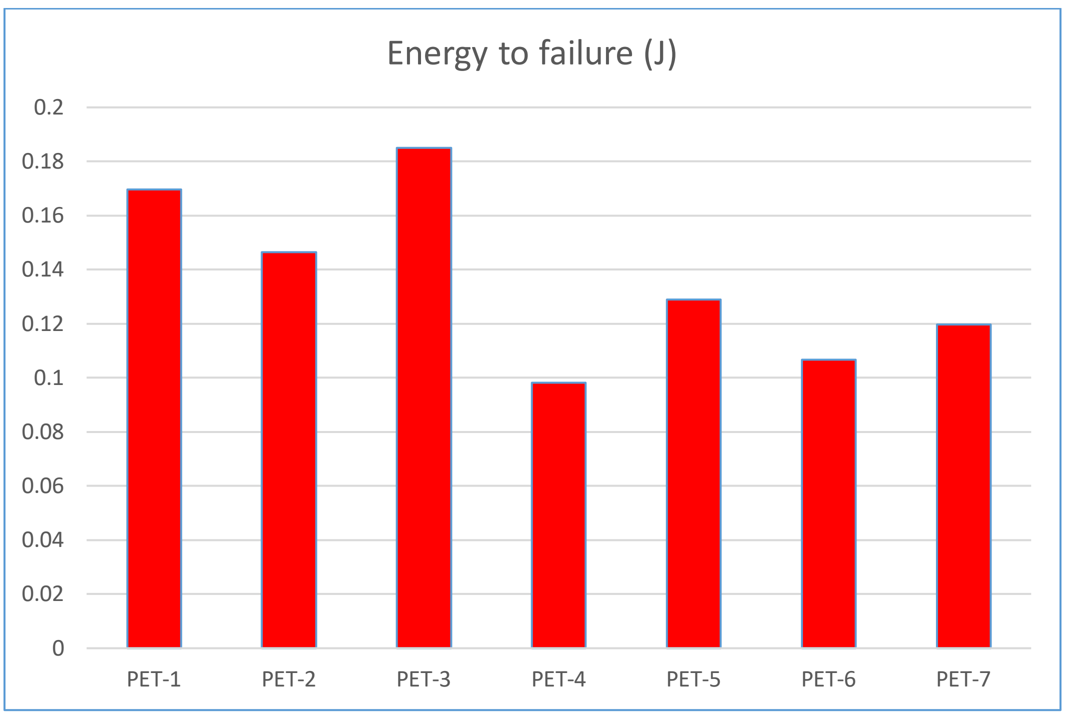

Fig. 29 Impact results of the PET-G specimens

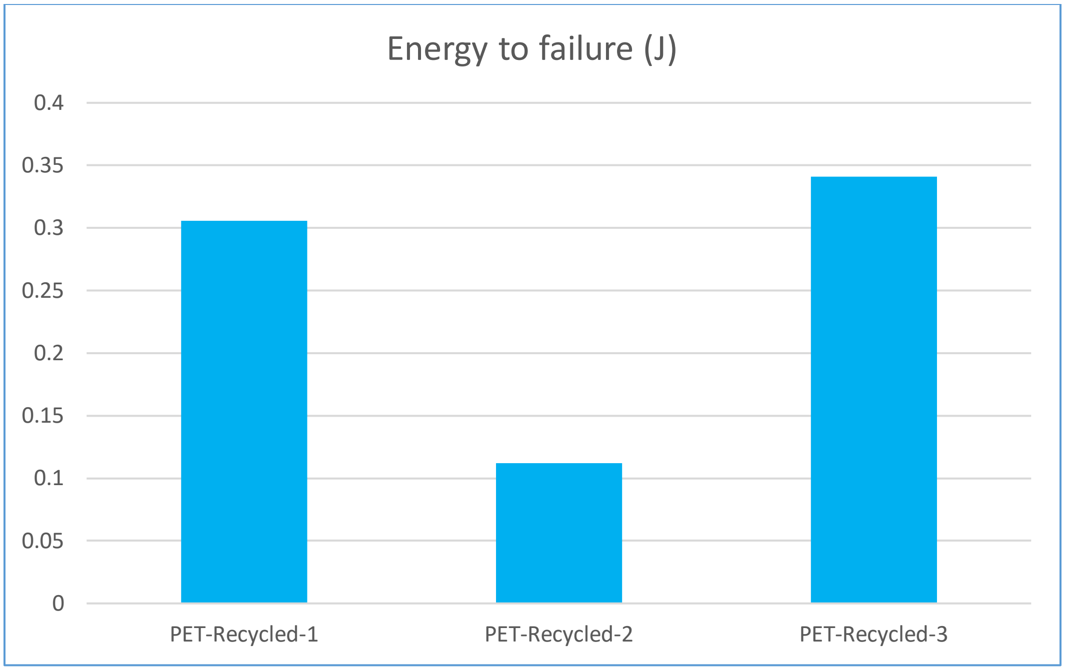

Fig. 30 Impact results of the rPET specimens

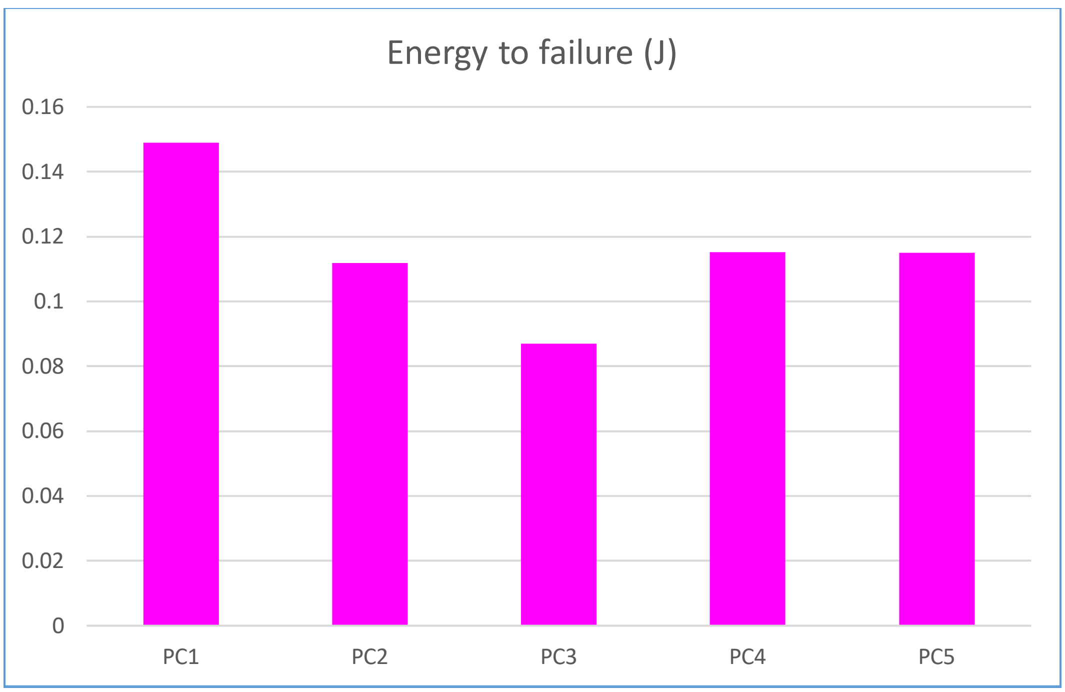

Fig. 31 Impact results of the PC specimens

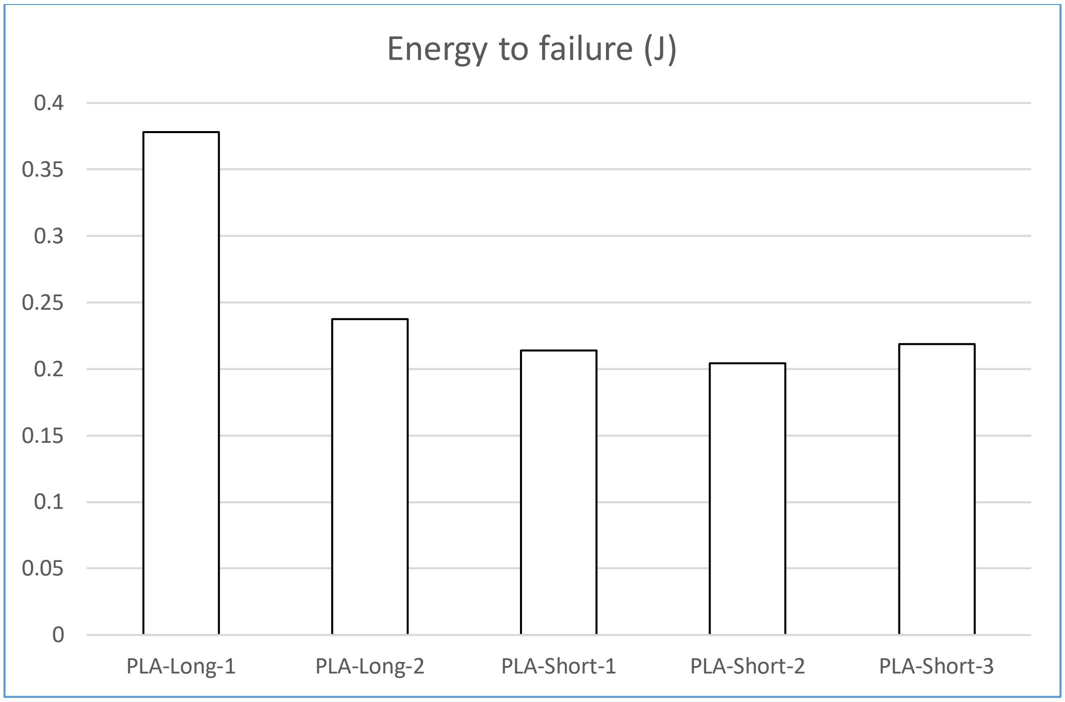

Fig. 32 Impact results of the PLA specimens

Table 2 Charpy impact testing results

Test No.	Impact velocity (m/s)	Specimen ID	Drop Weight (kg)	Time to max load (ms)	Maximum load (N)	Impact energy (J)	Energy to max load (J)	Total energy (J)	Energy to failure (J)	Deflection at failure (mm)	Total deflection (mm)
1	1.9912	ABS-1	4.8182	0.6653	612.3	9.5522	0.2751	0.4118	0.4092	1.6272	1.673
2	1.9881	ABS-2	4.8182	0.531	585.1	9.5223	0.1931	0.3775	0.3745	1.4682	1.526
3	1.9902	ABS-3	4.8182	0.5005	595.9	9.5423	0.1991	0.4561	0.4524	1.5279	1.5927
4	1.9906	ABS-4	4.8182	0.636	1248.3	9.5458	0.7629	1.1399	1.132	1.6532	1.7226
5	1.9911	ABS-5	4.8182	0.4456	501.6	9.5503	0.0506	0.3106	0.3088	1.5946	1.6284
6	1.9931	ABS-6	4.8182	0.6348	598.2	9.5698	0.3397	0.4557	0.4536	1.5305	1.5689
SD									0.3038		
AVG									0.5218		
1	1.9921	ABS-Recycled-1	4.8182	0.6616	1145.2	9.5604	0.7741	1.2169	1.2062	1.8218	1.9348
2	1.9912	ABS-Recycled-2	4.8182	0.6543	1096.2	9.5516	0.7545	1.1104	1.1025	1.7222	1.8033
3	1.9912	ABS-Recycled-3	4.8182	0.6604	1062.6	9.5515	0.6972	1.1655	1.1158	1.9074	2.5328
4	1.9917	ABS-Recycled-4	4.8182	0.6396	1112.1	9.5562	0.6463	1.1603	1.1063	1.9275	2.4258
5	1.9934	ABS-Recycled-5	4.8182	0.5664	732.5	9.5733	0.4993	0.6929	0.6882	1.4885	1.5574
6	1.9907	ABS-Recycled-6	4.8182	0.6836	741.5	9.5471	0.4551	0.637	0.6335	1.6932	1.7408
SD									0.2472		
AVG									0.9754		
1	1.9918	PET-1	4.8182	0.3796	317.7	9.5573	0.1206	0.171	0.1697	0.9841	1.0305
2	1.9929	PET-2	4.8182	0.3186	333.6	9.5685	0.1003	0.1478	0.1465	0.8383	0.8774
3	1.994	PET-3	4.8182	0.2942	408.5	9.5786	0.1197	0.1866	0.1850	0.8136	0.8526
4	1.9918	PET-4	4.8182	0.2698	273.9	9.5577	0.0652	0.0992	0.0982	0.7135	0.7453
5	1.9935	PET-5	4.8182	0.3064	306.1	9.5742	0.0868	0.1299	0.1289	0.8119	0.8461
6	1.9928	PET-6	4.8182	0.2539	260.8	9.5671	0.0678	0.1074	0.1066	0.7235	0.7578
7	1.9923	PET-7	4.8182	0.3186	299.3	9.5619	0.0826	0.1208	0.1198	0.8188	0.8531
SD									0.0323		
AVG									0.1364		
1	1.991	PET-Recycled-1	4.8182	0.4163	611.1	9.5494	0.2065	0.3078	0.3056	1.0597	1.1008
2	1.9905	PET-Recycled-2	4.8182	0.47	331.4	9.5454	0.0536	0.1137	0.1120	1.1917	1.2406
3	1.9918	PET-Recycled-3	4.8182	0.4419	623.6	9.5573	0.2339	0.3437	0.3408	1.1283	1.1791
SD									0.1232		
AVG									0.2528		
1	1.9892	PLA-Long-1	4.8182	0.4565	612.8	9.5324	0.2859	0.3812	0.3783	1.1285	1.1839
2	1.9892	PLA-Long-2	4.8182	0.3687	478.5	9.5322	0.1273	0.2402	0.2376	1.0712	1.1294
1	1.9915	PLA-Short-1	4.8182	0.2454	464.5	9.5548	0.1215	0.2157	0.2140	0.7528	0.7917
2	1.991	PLA-Short-2	4.8182	0.3015	639	9.55	0.123	0.2067	0.2043	0.7851	0.824
3	1.9901	PLA-Short-3	4.8182	0.3894	658.2	9.5415	0.137	0.2212	0.2187	0.9583	0.9971
SD									0.0724		
AVG									0.2506		
1	1.9888	PC1	4.8182	0.481	412.7	9.5286	0.0862	0.1506	0.1490	1.1834	1.2273
2	1.9893	PC2	4.8182	0.3882	238.1	9.5332	0.079	0.1127	0.1119	0.9732	1.0073
3	1.986	PC3	4.8182	0.437	270.1	9.5022	0.0557	0.0876	0.0869	1.0375	1.0667
4	1.9902	PC4	4.8182	0.4321	293	9.5418	0.0766	0.1162	0.1152	1.0541	1.0908
5	1.9871	PC5	4.8182	0.4651	293	9.5123	0.0709	0.1161	0.1151	1.1432	1.1846
SD									0.0221		
AVG									0.1156		

4.5 Three-Point Bend Testing

The three-point bend testing was performed on an Instron Model 1125 electromechanical machine, in accordance with ASTM D790.[11] Figure 33 shows a representative specimen within the three-point bend fixture. The purpose of this testing was to compare the as-built specimen properties to those subjected to UV exposure. The testing span between the lower pins was 60 mm, and the pin diameters were 6.35 mm. The loading rate used for testing was 1.7 mm/min, and the maximum displacement was 15 mm. The yield stress utilized was the 0.2% offset yield stress. Figures 34–36 represent the as-built flexural yield, flexural ultimate stress, and flexural modulus properties, respectively. Flexural modulus is the ratio of stress to strain in flexural deformation, with the higher results showing a tendency for a material to resist bending. Figures 37–39 show the results of the three-point bend testing of specimens subjected to UV exposure, compared to the as-built properties. PC results are only for as-built, as time constraints precluded UV exposure for these specimens. The results showed that as-built, PLA showed the best resistance to bending, followed by ABS, rPET, PET-G, and rABS. After UV exposure, each polymer showed a decrease in flexural yield stress and ultimate stress, except for the rABS material, which showed a slight increase in each of these properties. The flexural modulus after UV exposure increased for ABS and rABS, but decreased for all other polymers. The flexural modulus (resistance to bending) after UV exposure was highest for PLA, followed by ABS, r-PET, rABS, and PET-G.

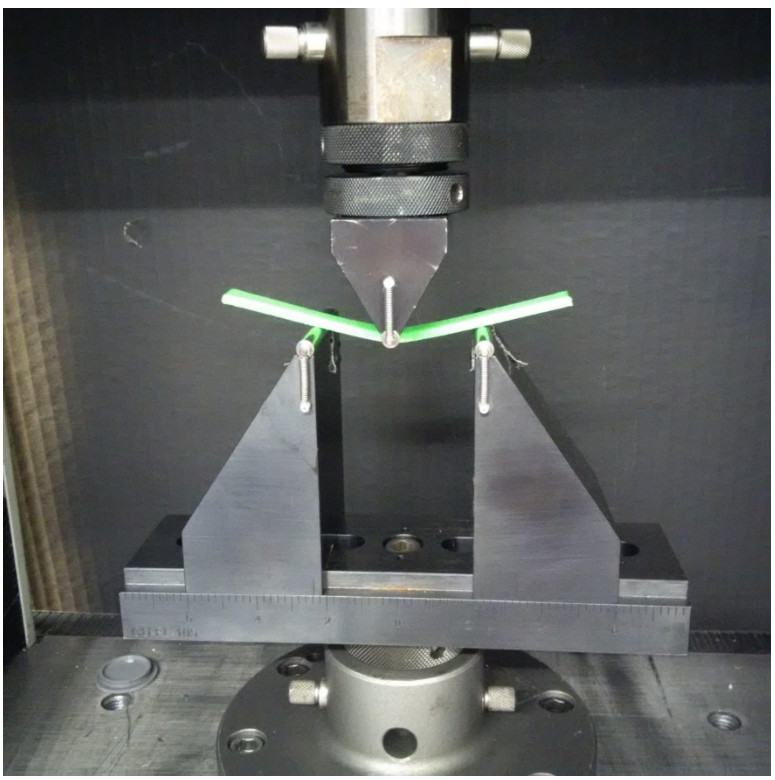

Fig. 33 Representative specimen within the three-point bend test fixture

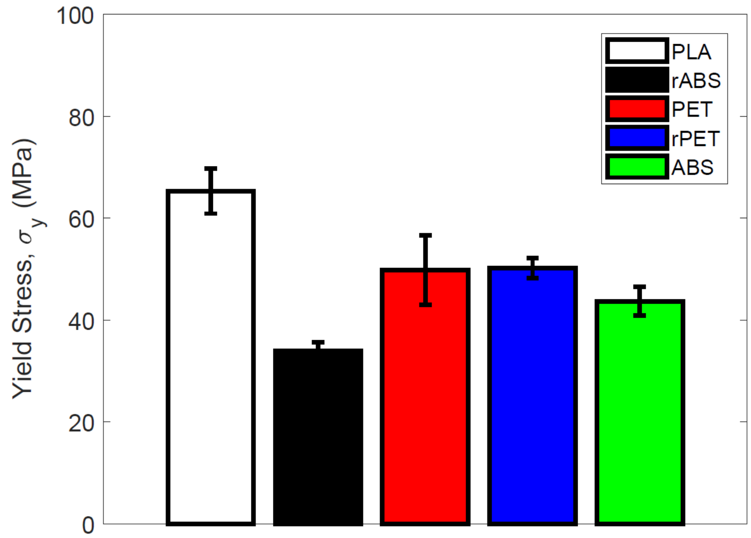

Fig. 34 Results of the three-point bend testing flexural yield stress

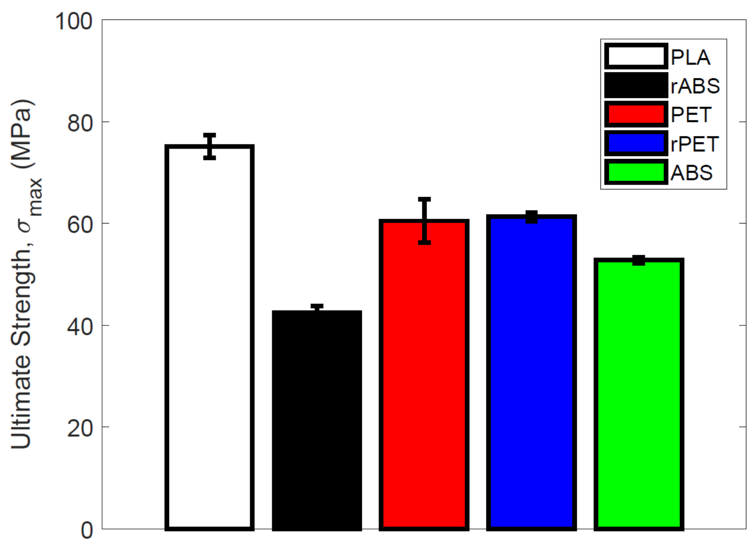

Fig. 35 Results of the three-point bend testing flexural ultimate stress

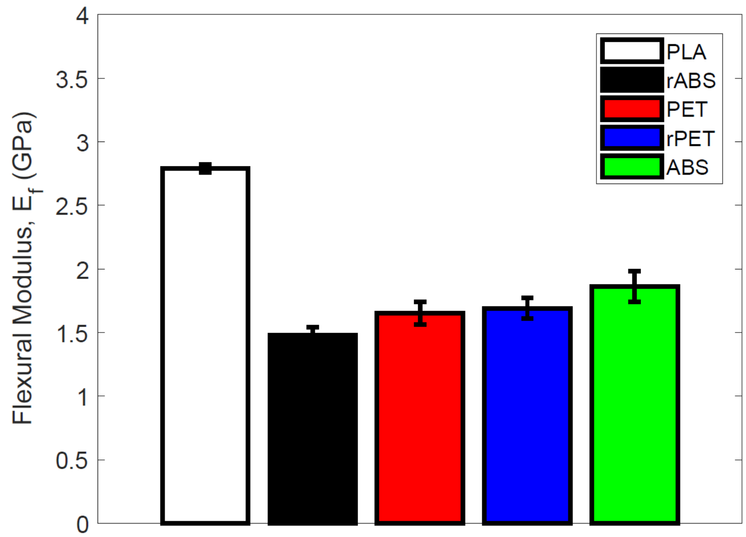

Fig. 36 Results of the three-point bend testing flexural modulus

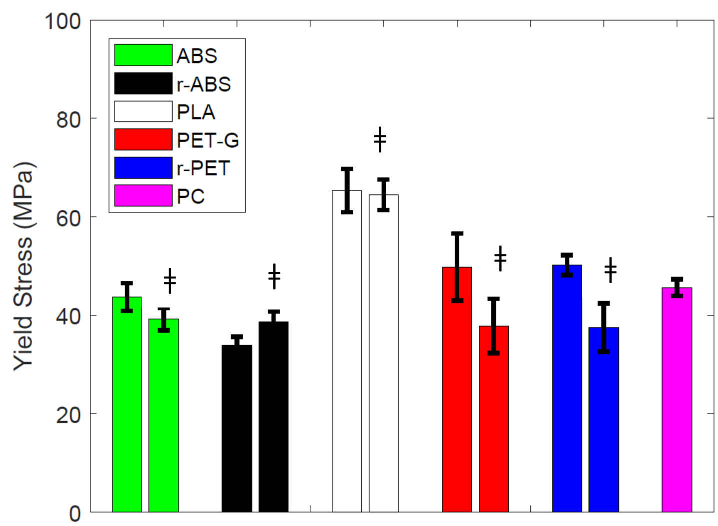

Fig. 37 Results of the three-point bend testing flexural yield stress for as-built (left bar) and UV exposed (ǂ) (right bar). Results for PC are only for as-built specimens.

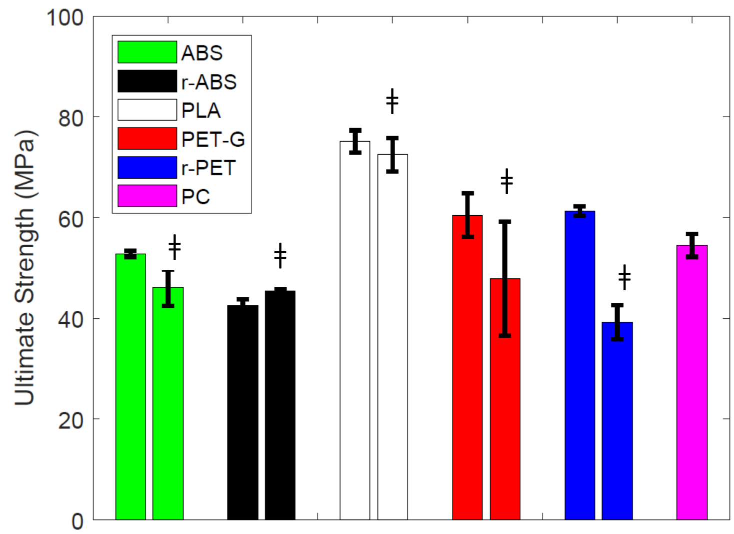

Fig. 38 **Results of the three-point bend testing ultimate stress for as-built (left bar) and UV exposed (ǂ) (right bar). Results for PC are only for as-built specimens.**

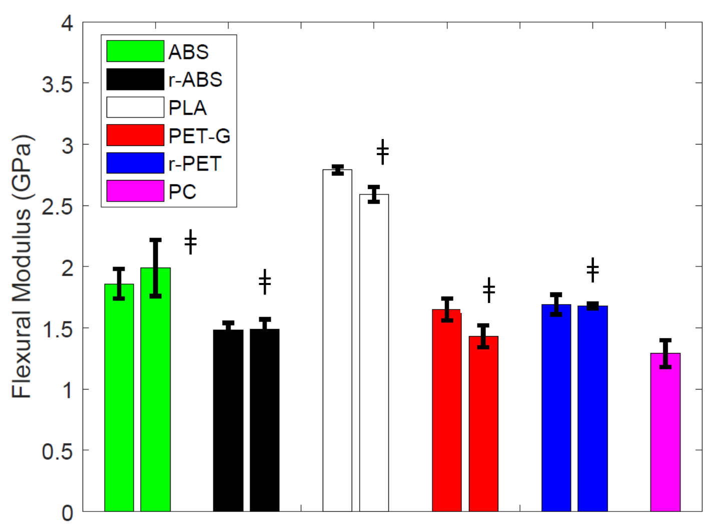

Fig. 39 **Results of the three-point bend testing flexural modulus for as-built (left bar) and UV exposed (ǂ) (right bar). Results for PC are only for as-built specimens.**

5. Fracture Surface Characterization through Optical Macroscopy

The fracture surfaces of the tensile and impact specimens were documented using optical macroscopy to note the features present after testing. The same build pattern was used for each polymer for the tensile and impact specimens. The observations contained within Sections 5.1 and 5.2 summarize the findings.

5.1 Tensile Specimen Fracture Surfaces

ABS (representative macrophotograph in Fig. 40) exhibited the following:

- Small pores notes on surface, approximately 100 μm in diameter, which represented the area between layer depositions.
- Less material toward edges and corners, more material toward center of specimen surface.
- Dark green and glass-like surface toward edges.

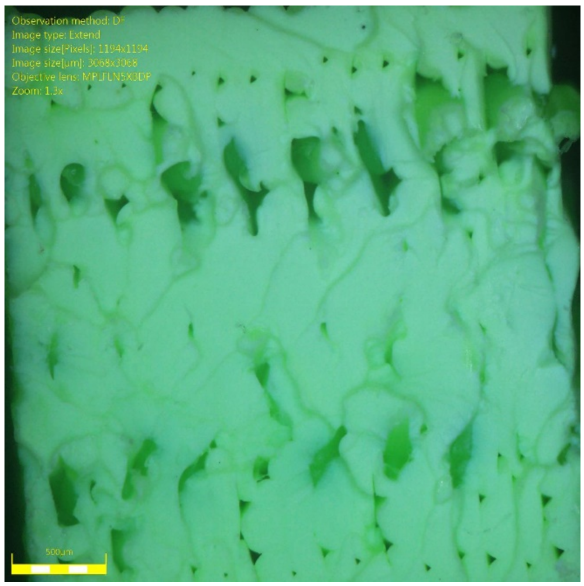

Fig. 40 Representative as-built ABS tensile specimen fracture surface. Scale bar = 500 μm

rABS (representative macrophotograph in Fig. 41) exhibited the following:

- Uneven surfaces, although the UV-exposed and water-immersed specimens appear more even.
- Edges and corners not connected.
- Surface is a lighter gray toward the center of the surface.

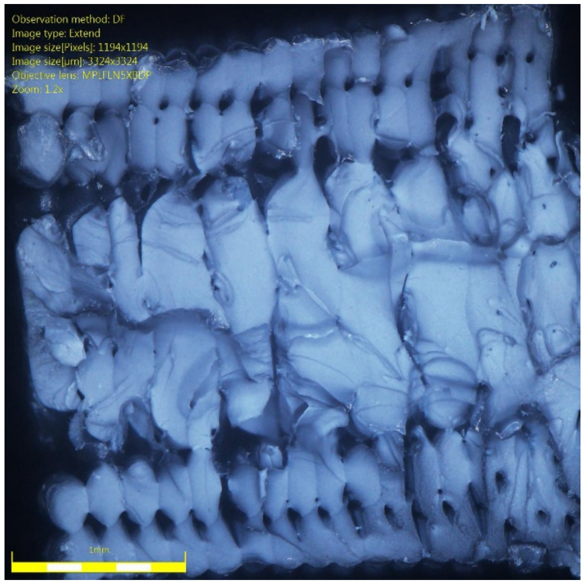

Fig. 41 Representative as-built rABS tensile specimen fracture surface. Scale bar = 1 mm.

PET-G (representative macrophotographs in Figs. 42 and 43) exhibited the following:

- Surface of as-built, UV-exposed and water immersed specimens showed evidence of conchoidal fracture, typical of glass fracture features.
- Orange discoloring noted.
- UV-exposed specimens showed longer fibers and darker red coloring, while water immersed specimens exhibited even longer fibers.

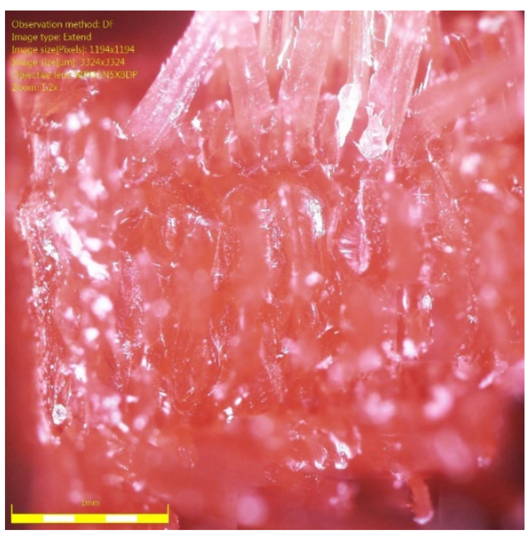

Fig. 42 Representative as-built PET-G tensile specimen fracture surface. Note the fibers extending from top surface. Scale bar = 1 mm.

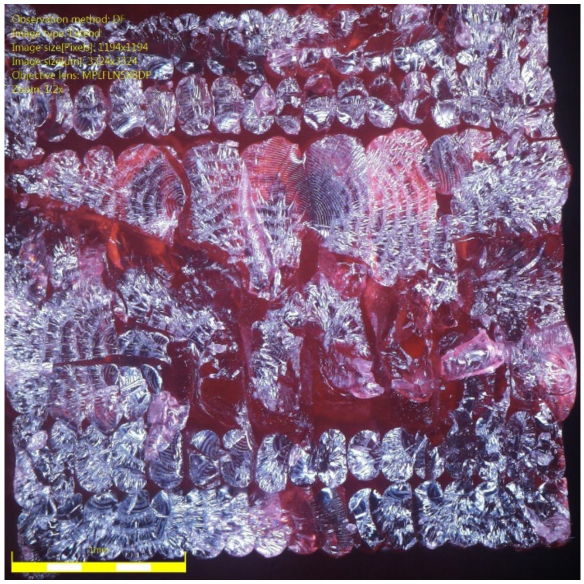

Fig. 43 Representative PET-G tensile specimen fracture surface subjected to water immersion. Note the conchoidal fracture demarcations. Scale bar = 1 mm.

rPET (representative macrophotograph in Fig. 44) exhibited the following:

- Showed evidence of fibers similar to PET-G fracture surfaces.
- Glass-like fracture surface.

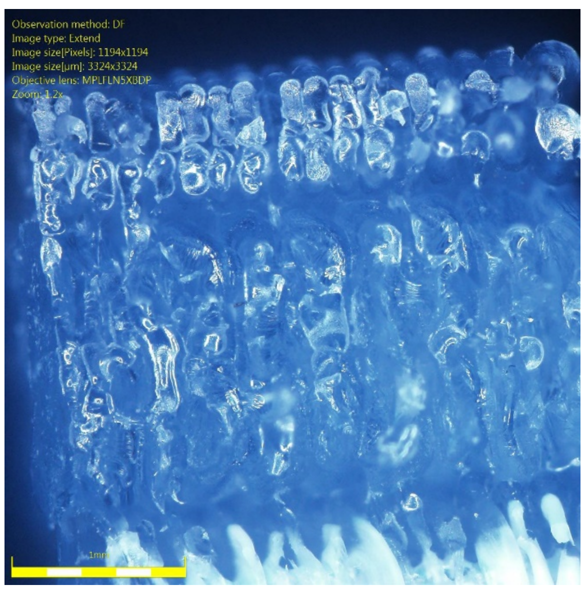

Fig. 44 Representative as-built rPET tensile specimen fracture surface. Scale bar = 1 mm.

PLA (representative macrophotographs in Figs. 45 and 46) exhibited the following:

- Edges and corners not connected.

- No pattern existed in the center of the specimens.
- UV-exposed specimens had smaller diameter pores.

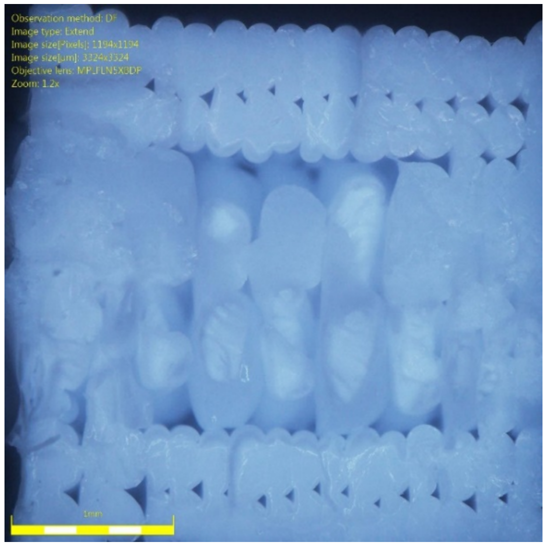

Fig. 45 Representative as-built PLA tensile specimen fracture surface. Scale bar = 1 mm.

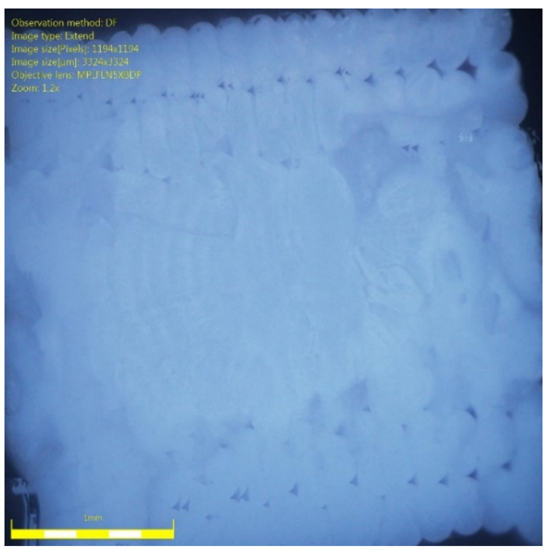

Fig. 46 Representative UV-exposed PLA tensile specimen fracture surface. Note the smaller internal pores. Scale bar = 1 mm.

5.2 Impact Specimen Fracture Surfaces

ABS (representative macrophotographs in Figs. 47 and 48) exhibited the following:

- Large gaps between layer depositions; distinct columnar structure based upon build profile.
- Corners and edges were separate from columns.

- 1/5-mm gaps.

Fig. 47 Representative ABS impact specimen fracture surface. Structure represents the build pattern. Scale bar = 1 mm.

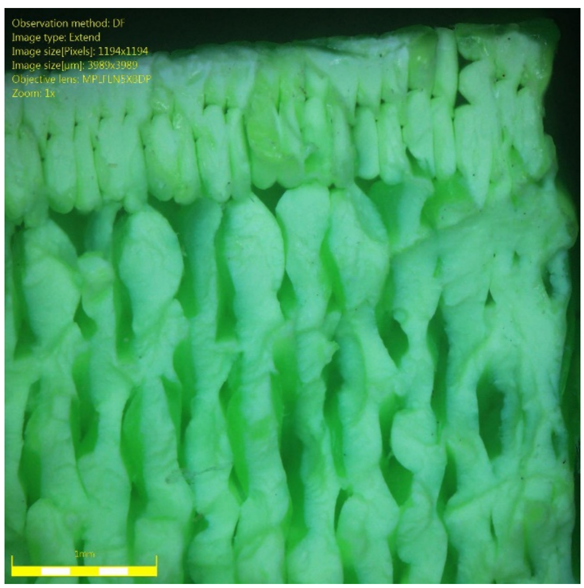

Fig. 48 Representative edge of ABS impact specimen fracture surface. Scale bar = 1 mm.

rABS (representative macrophotograph in Fig. 49) exhibited the following:

- Similar to fracture surface as ABS; large gaps between layer depositions; distinct columnar structure based upon build profile. Corners and edges were separate from columns.

- 3-mm gaps.

Fig. 49 Representative edge of rABS impact specimen fracture surface. Scale bar = 1 mm.

PET-G (representative macrophotographs in Figs. 50 and 51) exhibited the following:

- Corners and edges separate from fibers.
- Orange discoloring.
- Glass-like surfaces close to edges.
- Conchoidal fracture similar to tensile specimen fracture surfaces of PET-G.

Fig. 50 Representative PET-G impact specimen fracture surface showing internal orange discoloring. Scale bar = 1 mm.

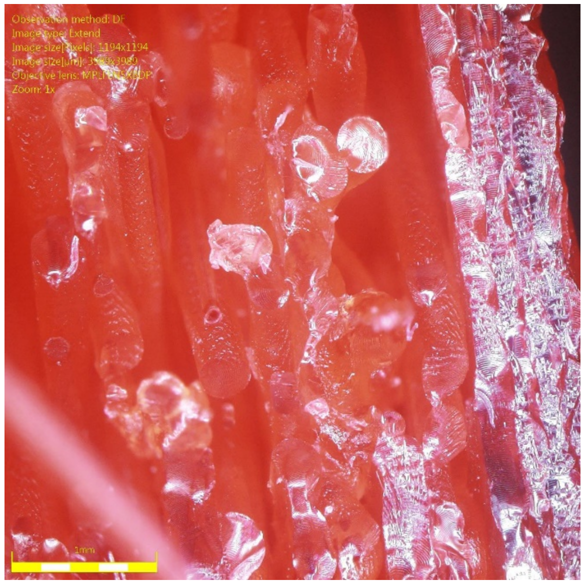

Fig. 51 Representative PET-G impact specimen fracture surface fibers and conchoidal fracture features. Scale bar = 1 mm.

rPET (representative macrophotographs in Figs. 52 and 53) exhibited the following:

- Glass-like surfaces close on corners and edges.
- Fibers noted on surface.
- Chunks missing from corners and edges.

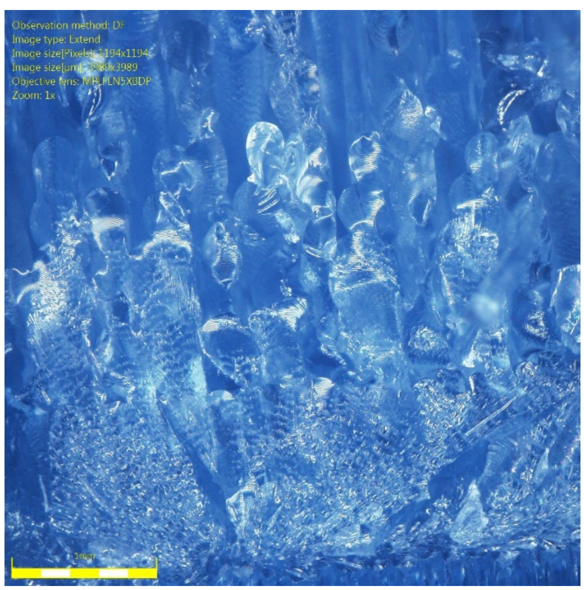

Fig. 52 Representative rPET impact specimen fracture surface showing fibers and conchoidal fracture. Scale bar = 1 mm.

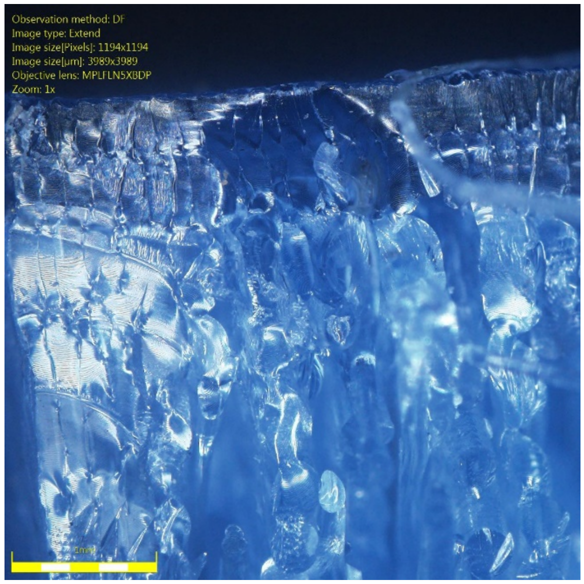

Fig. 53 Representative rPET impact specimen fracture surface showing glass-like fracture. Scale bar = 1 mm.

PLA (representative macrophotograph in Fig. 54) exhibited the following:

- Fewer gaps were noted as compared to other polymer impact specimens.

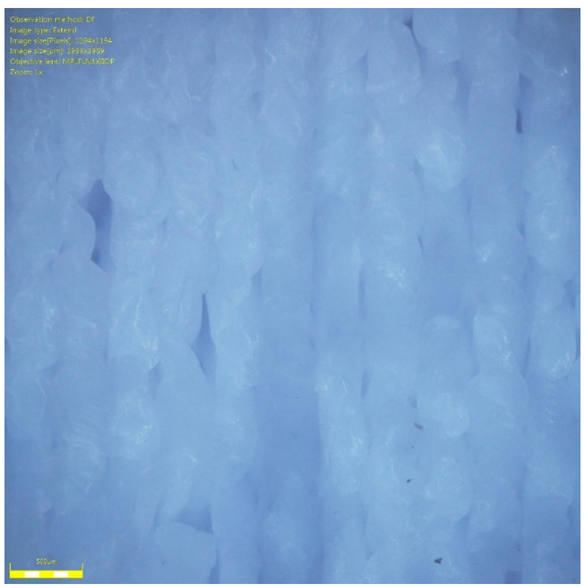

Fig. 54 Representative PLA impact specimen fracture surface. Scale bar = 1 mm.

PC (representative macrophotographs in Figs. 55 and 56) exhibited the following:

- Glass-like fracture features with minor divots and scratches.
- Lots of ridges; "snakeskin" features.

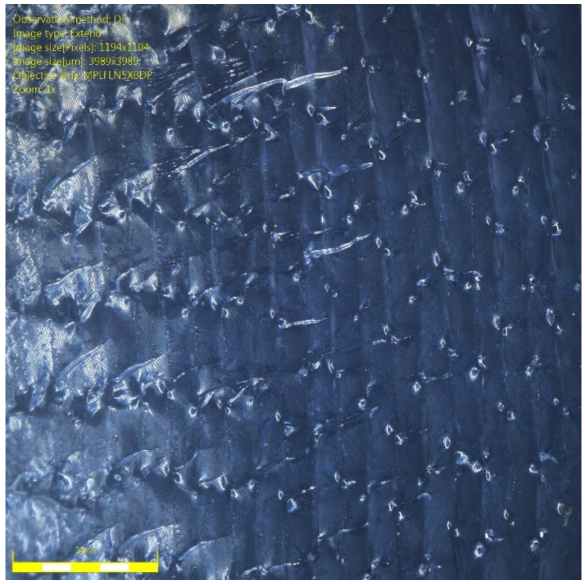

Fig. 55 Representative PC impact specimen fracture surface. Note the "snakeskin" appearance. Scale bar = 1 mm.

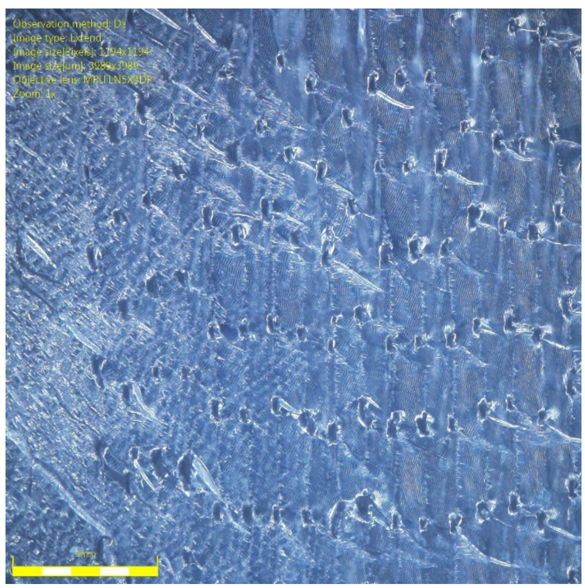

Fig. 56 Representative PC impact specimen fracture surface showing conchoidal glass-like fracture. Scale bar = 1 mm.

6. Discussion

It was obvious from the optical macroscopy work that the specimen fill could be optimized. It is expected that better properties could be realized with more complete builds, minimizing the internal cavities and pores. These pores act not only to reduce strength, but also could act to entrap moisture, further degrading mechanical properties. According to Galeta et al., the structure is the most significant factor and thereby has the strongest impact on the strength of 3-D printed models.[15] This is corroborated by Abbas et al., as well as Shubham et al., who showed that smaller layer thicknesses led to increased mechanical properties of 3-D-printed PLA specimens.[16,17] Therefore, future efforts should entail focusing on infill density and reduction of internal flaws that could weaken the as-built component.

In characterizing the fracture surfaces of the tensile specimens, it was clear that the ABS and rABS had the largest amount of internal voids, which most likely led to the lower tensile properties as compared to the other polymers. The opposite was true for impact results, albeit, on a small sampling of test specimens. Although the ABS and rABS impact specimens showed a similar amount of internal voids as the tensile specimens, the ABS and rABS exhibited the highest energy to failure. This may be due in part to the “brittle” features noted on many of the other impact fracture surfaces (i.e., PET-G, rPET, PC). It is presumed that the voids have more of an effect on tensile properties than impact properties of these polymers.

It was also noted that the recycled ABS and PET had higher impact values than the virgin ABS and PET-G (this trend was not seen with the tensile and three-point bend test results). This was interesting, because although PLA has been shown to be recyclable up to 10 times with little mechanical property degradation,[18,19] one study showed that 3-D-printed recycled ABS showed 13%–49% decrease in UTS and 17%–28% decrease in elastic modulus, depending on the print orientation.[20] Similar studies including recycled PET could not be found as of this writing.

Further testing using a statistically significant number of specimens is suggested to verify the impact properties of the recycled polymers.

Although UV exposure led to lower tensile strengths, as anticipated, it was interesting to note that specimens subjected to water immersion had little to no effect on tensile strength, and in some cases (i.e., for rABS and rPET), the tensile strength was greater for the water immersed specimens. Future work could focus on rheology testing after water immersion to further characterize these materials. It was noted that the recycled variants showed these trends, while their virgin counterparts did not. In addition, the tensile modulus for water-immersed ABS, rABS, and rPET all showed improvements over the non-immersed specimens. This contradicts studies that showed that moisture led to a reduction in polymer properties.[21,22] Again, further testing would be needed to verify these results.

7. Summary of Results

The following is a summary of the test results contained herein:

7.1 Water Immersion Testing

- The rABS, PET-G and rPET specimens exhibited the most weight gain as a result of water immersion testing, followed by PLA and ABS.

7.2 Tensile Testing

- The PLA specimens showed the highest as-built UTS, followed by PET-G, PC, rPET, ABS, and rABS.
- The PLA specimens also exhibited the highest tensile elastic modulus in the as-built condition, followed by PET-G, rPET, ABS, PC, and rABS.
- The tensile specimens subjected to UV exposure showed decreased UTS for each polymer tested, as well as decreased elastic modulus, except for the rABS specimens.
- The tensile specimens subjected to water immersion showed little to no difference in UTS for the ABS, rABS, and PLA specimens, as compared to as-built properties. The PET-G specimens showed a slightly lower UTS, while the UTS of the rPET specimens increased. The elastic modulus of water-immersed specimens was higher for ABS, rABS, and rPET (compared to as-built), while lower for PLA and PET-G.

7.3 Three-Point Bend Testing

- The PLA specimens exhibited the highest flexural yield stress in the as-built condition, followed by rPET, PET-G, PC, ABS, and rABS.
- The PLA specimens exhibited the highest flexural ultimate stress in the as-built condition, followed by rPET, PET-G, PC, ABS, and rABS.
- The PLA specimens exhibited the highest flexural modulus in the as-built condition, followed by ABS, rPET, PET-G, rABS, and PC.
- After UV exposure, the PLA showed the smallest decrease in flexural yield stress, followed by ABS, PET-G, and rPET. The rABS actually showed increased flexural yield stress as a result of UV exposure.

- After UV exposure, the PLA showed the smallest decrease in flexural ultimate stress, followed by ABS, PET-G, and rPET. Again, the rABS showed an increase in properties as a result of UV exposure.
- After UV exposure, the PLA and PET-G showed a decrease in flexural modulus, while the ABS, rABS, and rPET showed slight gains.

7.4 Charpy Impact Testing

- This testing showed a lot of variability within the test results, and only a few samples of each material were tested.
- The following is the order of decreasing energy to failure: rABS, ABS, PLA, rPET, PET-G, and PC.

8. Conclusion

A review of the final results would lead the reader to believe that PLA would be a great choice for 3-D-printed tools at the point of need. It showed a good combination of mechanical properties, and UV-exposure and water immersion had little to no effect on test results. However, PLA would probably not make the best choice of material for use in austere environments. When compared to ABS, it has a lower melting temperature, which means that use or storage in hot conditions may lead to warping and cracking. Based on this, ABS would probably be a better choice for this application, since it would be more suited for mechanical use since it is more resistance to the elements. However, it would also depend on the application—ABS has better impact properties, but PET-G and rPET have better tensile and bending properties.

New materials for 3-D printing are being introduced all of the time, and advanced high-strength materials not studied herein include acrylonitrile styrene acrylate (ASA), polyethylenimine (PEI), Ultem, polyether ether ketone (PEEK), Nylon 12, polyphenylsulfone (PPSF: also known as PPSU), and thermoplastic polyurethane (TPU), as well as composite polymers reinforced with carbon and alumina fibers and whiskers. Future work should entail research in these materials to determine feasibility of using them for point-of-need tools. When it comes to the vast array of items and potential of 3-D printing at the point of need, "The only limitation is our imagination".[5]

9. References

1. Kelly K. Need it fast? Marines can print it. Washington (DC): Marine Corps (US); 2018 Apr 26 [accessed 2019 July 26]. https://www.marines.mil/News/News-Display/Article/1503720/need-it-fast-marines-can-print-it.
2. SquatchSlaya. 3D printing on the battlefield. West Point (NY): Military Logistics Blog; 2014 Mar 3 [accessed 2019 July 26]. https://ds385.blogspot.com/2014/03/3d-printing-on-battlefield-additive.html.
3. Jeckell J. 3D printing: imagine a brigade producing parts on battlefield. Breaking Defense; 2014 Jan 14 [accessed 2019 July 26]. https://breakingdefense.com/2014/01/3d-printing-imagine-a-brigade-producing-parts-on-battlefield/.
4. Asclipiadis A. Rapid Equipping Force uses 3-D printing on the frontline. Washington (DC): Army (US); 2014 July 9 [accessed 2019 July 26]. https://www.army.mil/article/129635/Rapid_Equipping_Force_uses_3_D_printing_on_the_frontline/.
5. Fichtl M. Army field tests 3D-printing capabilities in South Korea. Stars and Stripes; 2018 Oct 29 [accessed 2019 July 26]. https://www.stripes.com/news/pacific/army-field-tests-3d-printing-capabilities-in-south-korea-1.554269.
6. Giang K. PLA vs. ABS: what's the difference? 3D Hubs; 2019 [accessed 2019 July 26]. https://www.3dhubs.com/knowledge-base/pla-vs-abs-whats-difference.
7. Alexandrea P. 3D printer materials guide: 3D printing plastics. 3D Natives; 2018 Feb 23 [accessed 2019 July 26]. https://www.3dnatives.com/en/plastics-used-3d-printing110420174.
8. 3d Matter. FDM 3D Printing materials compared. 3D Hubs; n.d. [accessed 2019 July 26]. https://www.3dhubs.com/knowledge-base/fdm-3d-printing-materials-compared.
9. ASTM E8. Standard test method for tension testing of metallic materials. West Conshohocken (PA): ASTM International; 2016.
10. ASTM D6110. Standard test method for determining charpy impact resistance of notched specimens of plastics. West Conshohocken (PA): ASTM International; 2018.

11. ASTM D790. Standard test methods for flexural properties of unreinforced and reinforced plastics and electrical insulating materials. West Conshohocken (PA): ASTM International; 2017.
12. ASTM G154. Standard practice for operating fluorescent ultraviolet (UV) lamp apparatus for exposure of nonmetallic materials. West Conshohocken (PA): ASTM International; 2016.
13. ASTM G151. Standard practice for exposing nonmetallic materials accelerated test devices that use laboratory light sources. West Conshohocken (PA): ASTM International; 2019.
14. ASTM D2842. Standard test method for water absorption of rigid cellular plastics. West Conshohocken (PA): ASTM International; 2019.
15. Galeta T, Brod S, Somolanji M. Impact of structure and building orientation on strength of 3D printed models. Kautschuk gummi kunststoffe (KGK). 2012;65(10):36–42. https://www.tib.eu/de/suchen/id/BLSE%3ARN320332459/Impact-of-Structure-and-Building-Orientation-on/.
16. Abbas TF, Othman FM, Ali HB. Influence of layer thickness on impact property of 3D-printed PLA. International Research Journal of Engineering and Technology (IRJET). 2018 Feb;05(02).
17. Shubham P, Sikidar A, Chand T. The influence of layer thickness on mechanical properties of the 3D printed ABS polymer by fused deposition modeling. Key Engineering Materials. 2016 Aug.
18. Anderson I. Mechanical properties of specimens 3D printed with virgin and recycled polyactic acid. 3D Printing and Additive Manufacturing Journal. 2017 June;4(2):1.
19. Pakkanen J, Manfredi D, Minetola P, Iuliano L. About the use of recycled or biodegradable filaments for sustainability of 3D printing. Proceedings of Smart Innovation Conference; 2017 Apr.
20. Mohammed IM. EcoPrinting: Investigating the use of 100% recycled Acrylonitrile Butadiene Styrene (ABS) for additive manufacturing. Proceedings from the 28th Solid Freeform Fabrication Conference; 2017.
21. Walter H, Shirangi H, Wunderle B, Demitzaki E. Study on the effect of moisture and elevated temperature on the fracture properties of viscoelastic polymers. Proc Int Conf Fracture (ICF12); 2009 July; Ottawa, Canada.

22. Jabarin SA, Lofgren EA. Effect of water absorption on physical properties of high nitrile barrier polymers. Polymer Engineering and Science. 1986 Mar;26(6).

List of Symbols, Abbreviations, and Acronyms

3-D	three-dimensional
ABS	acrylonitrile butadiene styrene
AM	additive manufacturing
ARL	Army Research Laboratory
ASA	acrylonitrile styrene acrylate
CCDC	Combat Capabilities Development Command
ExLab	Expeditionary Laboratory
FOB	forward-operating base
MWTC	Mountain Warfare Training Center
PC	polycarbonate
PEEK	polyether ether ketone
PEI	polyethylenimine
PET-G	glycol modified polyethylene terephthalate
PLA	polylactic acid
PPSF (PPSU)	polyphenylsulfone
rABS	recycled ABS
rPET	recycled PET
REF	Rapid Equipping Force
RFAB	Rapid Fabrication via Additive Manufacturing on the Battlefield
STL	stereolithography
TPU	thermoplastic polyurethane
UTS	ultimate tensile strength
UV	ultraviolet
WMRD	Weapons and Materials Research Directorate

1 (PDF) DEFENSE TECHNICAL INFORMATION CTR
DTIC OCA

1 (PDF) CCDC ARL
FCDD RLD CL
TECH LIB

1 (PDF) CCDC ARL
FCDD RLW MD
M PEPI